

Complex of $\beta 4$ GalT-II and GlcAT-P in HNK-1 Biosynthesis

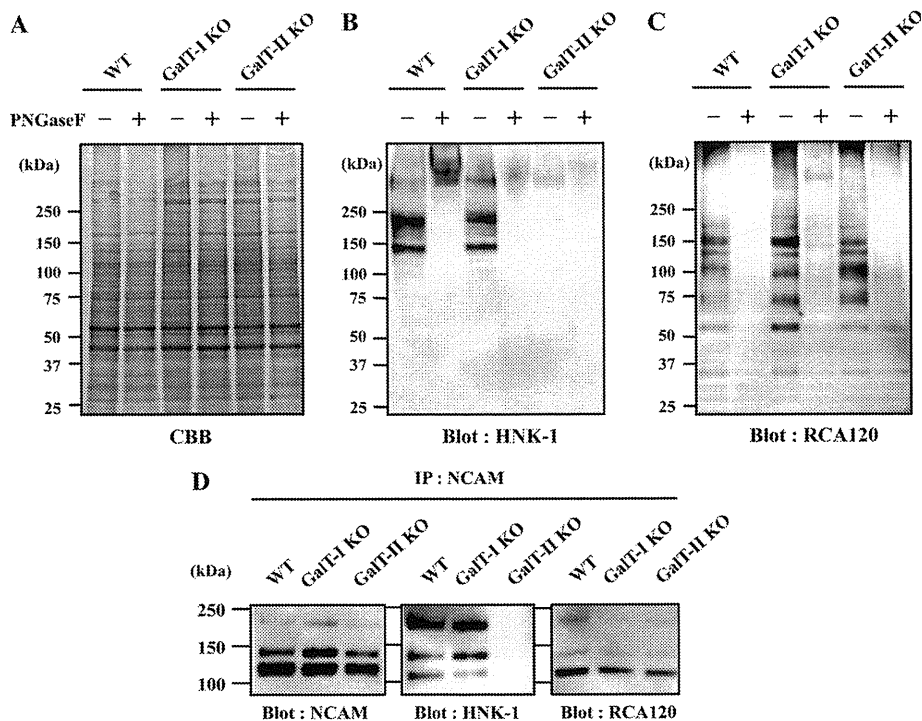


FIGURE 1. **Expression of HNK-1 carbohydrate and *N*-acetylglucosamine in mouse brains.** Membrane fractions of 4-week-old C57BL/6 (WT), $\beta 4$ GalT-I-deficient (GalT-I-KO), and $\beta 4$ GalT-II-deficient (GalT-II-KO) mouse brain were subjected to SDS-PAGE followed by Coomassie Brilliant Blue (CBB) staining (A), Western blotting with HNK-1 mAb (B), or lectin blotting with RCA120 (C). D, membrane fractions of 4-week-old mouse brains were immunoprecipitated (IP) with anti-NCAM antibody, subjected to SDS-PAGE, and blotted with anti-NCAM mAb, HNK-1 mAb, and RCA120. PNGase F, peptide-*N*-glycosidase F.

HNK-1 (19, 20). To directly compare the expression of HNK-1 in these mutant mice, brain membrane fractions were prepared from wild-type and $\beta 4$ GalT-I, II-deficient mice (Fig. 1A) and Western-blotted with the HNK-1 mAb (Fig. 1B). Consistent with previous reports, HNK-1 expression was dramatically decreased in $\beta 4$ GalT-II-deficient mice but was normal in $\beta 4$ GalT-I-deficient mice. Most HNK-1 epitopes in the wild-type mice disappeared after treatment with peptide *N*-glycosidase F (Fig. 1B, 2nd lane), indicating that HNK-1 carbohydrates are mainly expressed on *N*-glycan in the membrane fraction. This suggests that $\beta 4$ GalT-II synthesizes most HNK-1 carbohydrates on *N*-glycans in the brain. To explore the molecular mechanism involved, we first confirmed that the GlcAT-P transcript was expressed normally in these knock-out mice brains (supplemental Fig. 1). Next, to examine whether the *N*-acetylglucosamine residue remains in these knock-out mice, a lectin blot analysis was performed using RCA120, which predominantly recognizes the β Gal residue of *N*-acetylglucosamine. Because the nonreducing end of *N*-acetylglucosamine is often capped by sialic acid, the membrane was treated with sialidase prior to RCA120 blotting. As a result, $\beta 4$ GalT-I and -II-deficient mice showed similar reactivity for RCA120 to wild-type mice, most of which disappeared after peptide *N*-glycosidase F treatment, indicating that the *N*-acetylglucosamine on *N*-glycans was normally expressed in these knock-out mice and that several $\beta 4$ GalTs contribute to the biosynthesis of *N*-linked *N*-acetylglucosamine in the brain. This excludes the possibility that the reduction in HNK-1 is due to a general loss of *N*-acetylglucosamine in the $\beta 4$ GalT-II-deficient brain.

Another possibility is that $\beta 4$ GalT-II is the only $\beta 4$ GalT in HNK-1-expressing cell or a specific $\beta 4$ GalT for HNK-1 carrier proteins. To test this, we focused on NCAM. Because NCAM is a major carrier of HNK-1 carbohydrates in the nervous system, it must be expressed in HNK-1-positive cells. NCAM was immunoprecipitated from the brain membrane fraction and blotted with anti-NCAM mAb, HNK-1 mAb, and RCA120. As shown in Fig. 1D, three major splicing isoforms of NCAMs (NCAM-120, NCAM-140, and NCAM-180) are detected, and no difference in expression levels of each NCAM isoform (Blot: NCAM) or in reactivity with *Ricinus communis* agglutinin (Blot: *R. communis* agglutinin was observed among three genotypes. In contrast, HNK-1 is predominantly expressed on NCAM-180 and NCAM-140 rather than on NCAM120 in wild-type mice brain, which is consistent with a previous report (30). The HNK-1 on NCAM disappeared in $\beta 4$ GalT-II-deficient mice (Blot: HNK-1). These results indicate that other $\beta 4$ GalTs synthesize *N*-acetylglucosamine even onto NCAM in $\beta 4$ GalT-II-deficient mice and also suggest that $\beta 4$ GalT-II is not the only enzyme in HNK-1-expressing cells and not responsible for the general production of *N*-acetylglucosamine on HNK-1 carrier molecules. Therefore, it is possible that GlcAT-P transfers glucuronic acid (GlcA) only to the *N*-acetylglucosamine structure that $\beta 4$ GalT-II synthesizes, prompting us to speculate that GlcAT-P specifically associates with $\beta 4$ GalT-II.

Co-immunoprecipitation of GlcAT-P and $\beta 4$ GalT-II—To investigate the interaction between $\beta 4$ GalT-II and GlcAT-P, we performed co-immunoprecipitation experiments. Myc-tagged $\beta 4$ GalT-I or -II ($\beta 4$ GalT-I-myc or $\beta 4$ GalT-II-myc) and

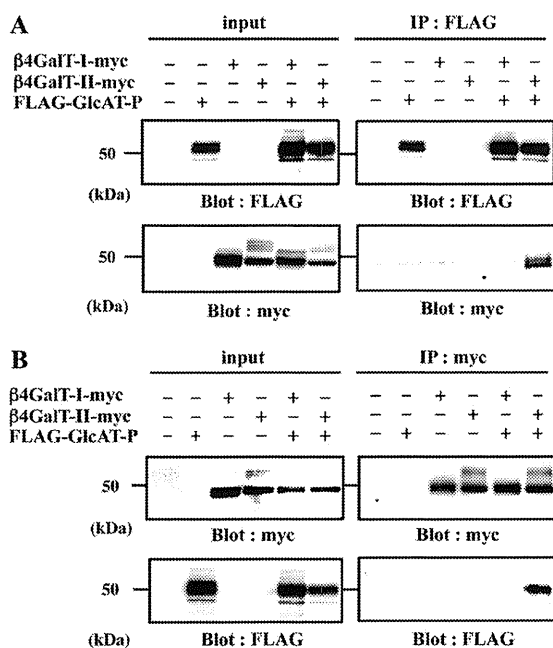


FIGURE 2. Co-immunoprecipitation of GlcAT-P and $\beta 4$ GalT-II in N2a cells. Lysate of N2a cells transiently expressing FLAG-GlcAT-P, $\beta 4$ GalT-I-myc, or $\beta 4$ GalT-II-myc was immunoprecipitated (IP) with anti-FLAG pAb (A, IP: FLAG) or anti-Myc pAb (B, IP: myc), subjected to SDS-PAGE, and Western-blotted (Blot) with anti-FLAG mAb or anti-Myc mAb. To examine the level of each protein, the cell lysates were directly subjected to SDS-PAGE and Western blotting with anti-FLAG mAb or anti-Myc mAb (input).

FLAG-tagged GlcAT-P (FLAG-GlcAT-P) were transiently expressed in N2a cells, and cell lysates were incubated with anti-FLAG pAb to precipitate FLAG-GlcAT-P (Fig. 2A, IP: FLAG). Subsequent Western blotting was conducted with anti-Myc mAb to detect $\beta 4$ GalT-I and -II-myc. As shown in Fig. 2A, right lower panel, $\beta 4$ GalT-II-myc was co-immunoprecipitated by FLAG-GlcAT-P, whereas $\beta 4$ GalT-I-myc was not. To determine whether FLAG-GlcAT-P could be conversely co-precipitated by $\beta 4$ GalT-II-myc, we conducted immunoprecipitation using anti-Myc pAb. As shown in Fig. 2B, right lower panel, FLAG-GlcAT-P was co-immunoprecipitated by $\beta 4$ GalT-II-myc, but not by $\beta 4$ GalT-I-myc. These results revealed that GlcAT-P specifically interacted with $\beta 4$ GalT-II in cells.

Effect of ER-retained GlcAT-P on $\beta 4$ GalT-II Localization—Next, we performed an ER-retention assay (6, 31) to visualize the interaction. Normally, GlcAT-P and $\beta 4$ GalT-I and -II mainly occur in Golgi, as was confirmed by co-localization with a Golgi marker, GM130, in N2a cells (supplemental Fig. 2). GlcAT-P appeared to co-localize with $\beta 4$ GalT-I as well as $\beta 4$ GalT-II under normal conditions (Fig. 3, B–G). In the ER-retention assay, we employed an ER-retained version of GlcAT-P in which a dibasic motif (K/R)(X)(K/R) was mutated (Fig. 3A). Some glycosyltransferases have this motif in their cytoplasmic tail, which is required for transport from the ER to the Golgi apparatus (32). Actually, GlcAT-P lacking this motif (GlcAT-P-AAA) was retained in the ER (Fig. 3, H and K, and also see supplemental Fig. 3, A and D) (16). To investigate the effect of GlcAT-P-AAA on the distribution of $\beta 4$ GalT-I and -II, N2a cells expressing GlcAT-P-AAA and $\beta 4$ GalT-I or -II-myc were immunostained. As a result, the location of $\beta 4$ GalT-II-myc

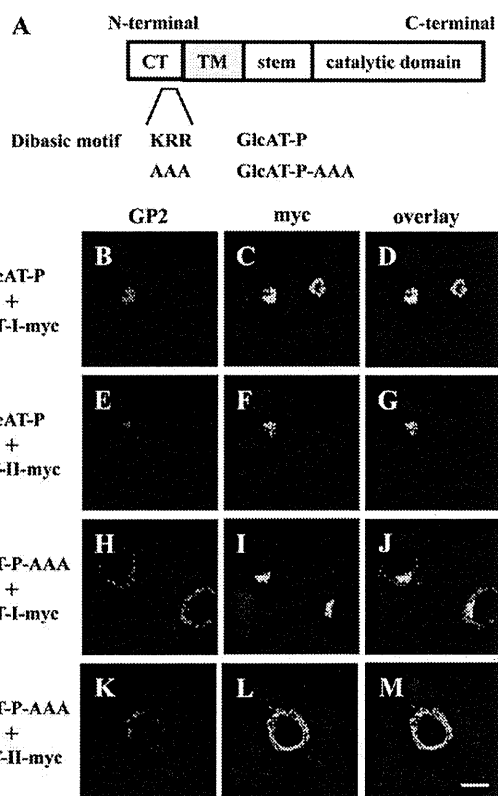


FIGURE 3. ER retention assays using GlcAT-P-AAA. A, schematic diagrams of GlcAT-P and GlcAT-P-AAA. CT, cytoplasmic tail, TM, transmembrane domain. B–M, N2a cells were transiently co-transfected with GlcAT-P or GlcAT-P-AAA and $\beta 4$ GalT-I-myc or $\beta 4$ GalT-II-myc. GlcAT-P and GlcAT-P-AAA were detected with GP2 pAb (B, E, H, and K) and Alexa 546-conjugated secondary antibodies. $\beta 4$ GalT-myc (I and II) was detected with anti-Myc mAb (C, F, I, and L) and Alexa 488-conjugated secondary antibodies. D, G, J, and M, overlaid images. Bar, 10 μ m.

changed to the ER from the Golgi (Fig. 3L and supplemental Fig. 3E), which overlapped with GlcAT-P-AAA (Fig. 3M and supplemental Fig. 3F), whereas $\beta 4$ GalT-I-myc was still localized to the Golgi regardless of the expression of GlcAT-P-AAA (Fig. 3, I and J, and also see supplemental Fig. 3, B and C). These results reinforce the notion of selective interaction between GlcAT-P and $\beta 4$ GalT-II in cells.

$\beta 4$ GalT-II and $\beta 4$ GalT-I Do Not Associate with PST—To examine the specificity of the binding between $\beta 4$ GalT-II and GlcAT-P, we used a PST instead of GlcAT-P. PST is one of the $\alpha 2,8$ -polysialyltransferases involved in the biosynthesis of PSA (33, 34), and PSA is attached to monosialylated *N*-acetylglucosamine on NCAM (35). Our previous study revealed that PSA was expressed in the brain of $\beta 4$ GalT-II-deficient mice at the same level as in wild-type mice (19). This is also the case in $\beta 4$ GalT-I-deficient mice (20). Therefore, we expected that $\beta 4$ GalT-I and -II would not associate with PST. $\beta 4$ GalT-I- or -II-myc and PST-FLAG were expressed in N2a cells, immunoprecipitated with anti-FLAG pAb, and subjected to Western blotting with anti-Myc mAb. As shown in Fig. 4, lower panel, $\beta 4$ GalT-I and -II were not co-precipitated with PST, suggesting that these enzymes do not interact in cells.

To support the immunoprecipitation data, an ER retention assay was performed using PST-AAA-FLAG (Fig. 5A), a mutant

Complex of $\beta 4\text{GalT-II}$ and GlcAT-P in HNK-1 Biosynthesis

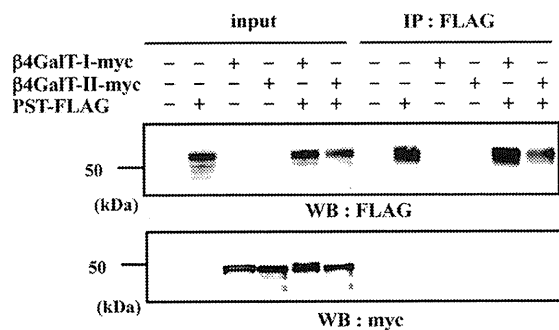


FIGURE 4. Immunoprecipitation using PST-FLAG and $\beta 4\text{GalT-myc}$ in N2a cells. Lysate of N2a cells transiently expressing PST-FLAG, $\beta 4\text{GalT-I-myc}$, or $\beta 4\text{GalT-II-myc}$ were immunoprecipitated (IP) with anti-FLAG pAb (IP: FLAG), subjected to SDS-PAGE, and Western-blotted with anti-FLAG mAb or anti-Myc mAb. To examine the level of each protein, the cell lysates were directly subjected to SDS-PAGE and then Western blotting (WB) with anti-FLAG mAb or anti-Myc mAb (input).

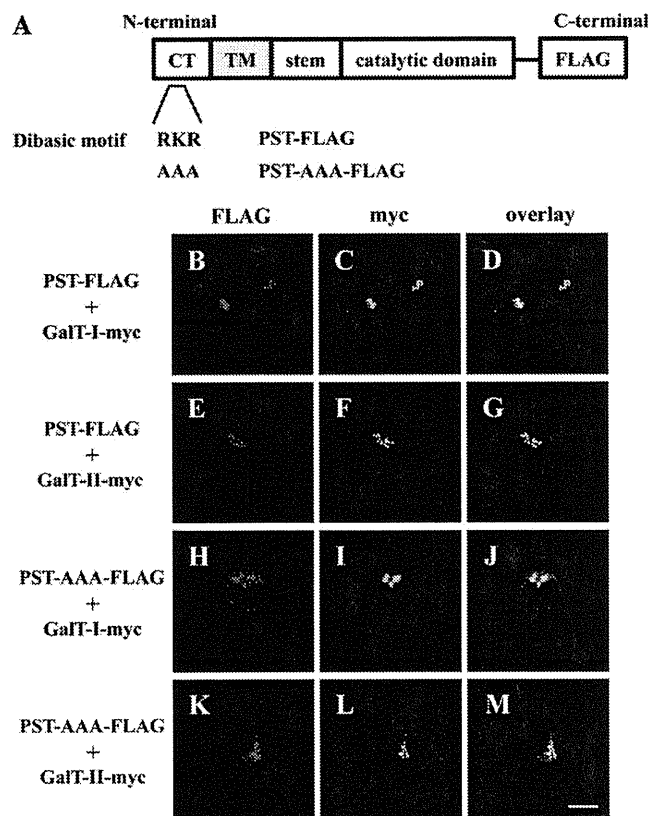


FIGURE 5. ER retention assays using PST-AAA-FLAG. A, schematic diagrams of PST-FLAG and PST-AAA-FLAG. B–M, N2a cells were transiently co-transfected with PST-FLAG or PST-AAA-FLAG and $\beta 4\text{GalT-I-myc}$ or $\beta 4\text{GalT-II-myc}$. PST-FLAG or PST-AAA-FLAG was detected with anti-FLAG pAb (B, E, H, and K), and Alexa 546-conjugated secondary antibodies. $\beta 4\text{GalT-myc}$ (I and L) was detected with anti-Myc mAb (C, F, I, and L) and Alexa 488-conjugated secondary antibodies. D, G, J, and M, overlaid images. Bar, 10 μm . CT, cytoplasmic tail, TM, transmembrane domain.

of the dibasic motif (K/R)(X)(K/R) in PST. PST is also localized to the Golgi apparatus, as confirmed by the co-localization of PST-FLAG with $\beta 4\text{GalT-I}$, and -II-myc in the Golgi (Fig. 5, B–G). As expected, the altered distribution of PST-AAA-FLAG was observed as shown in Fig. 5, H and K, and also in supplemental Fig. 3, G and J. The distribution of PST-AAA is slightly

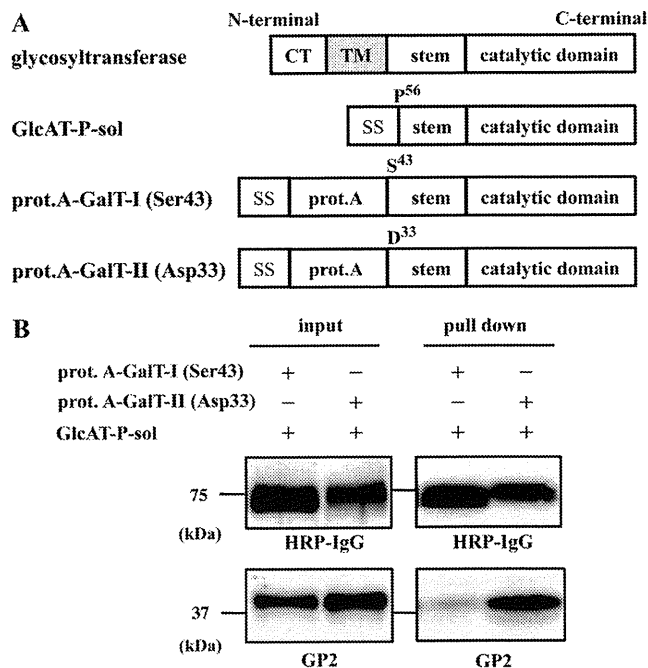


FIGURE 6. Pull-down assays using soluble forms of GlcAT-P-sol , prot.A-GalT-I , and prot.A-GalT-II . A, schematic diagrams of GlcAT-P-sol , prot.A-GalT-I (Ser-43), and prot.A-GalT-II (Asp-33). SS, signal sequence. B, culture medium of N2a cells transiently expressing GlcAT-P-sol and prot.A-GalT-I (Ser-43) or prot.A-GalT-II (Asp-33) was incubated with IgG-Sepharose TM6 Fast Flow (pull-down), subjected to SDS-PAGE, and Western-blotted with HRP-conjugated normal rabbit IgG or GP2 pAb. To examine the level of each protein, the culture medium was directly subjected to SDS-PAGE and then Western-blotted with HRP-conjugated normal rabbit IgG or GP2 pAb (input). CT, cytoplasmic tail, TM, transmembrane domain.

different from GlcAT-P-AAA , i.e. PST-AAA was detected not only in ER but in Golgi, suggesting that the effect of the mutation of dibasic motif on ER distribution varies by an individual glycosyltransferase as described previously (32). However, the altered distribution of PST-AAA did not perturb the Golgi-based localization of $\beta 4\text{GalT-I}$ and -II-myc (Fig. 5, I, J, L, and M, and also see supplemental Fig. 3, H, I, K, and L). These results revealed that $\beta 4\text{GalT-I}$ and -II do not associate with PST, supporting our idea that $\beta 4\text{GalT-II}$ and GlcAT-P form a specific complex.

Interaction between GlcAT-P and $\beta 4\text{GalT-II}$ through Their Luminal Domains—Glycosyltransferases, such as GlcAT-P and $\beta 4\text{GalT}$, are type II transmembrane proteins with a short cytoplasmic tail, a hydrophobic single-pass transmembrane domain, a stem region, and a catalytic domain (Fig. 6A) (36). We previously reported that GlcAT-P and HNK-1ST formed an enzyme complex through their catalytic domains in the Golgi lumen (37). Thus, we examined whether GlcAT-P and $\beta 4\text{GalT-II}$ also form a complex via their Golgi luminal domains. We constructed an expression vector encoding the luminal domain of GlcAT-P downstream of the insulin signal sequence (GlcAT-P-sol). Similarly, expression vectors for luminal domains of $\beta 4\text{GalT-I}$ and -II fused with the signal sequence and protein A (prot.A-GalT-I (Ser-43) and prot.A-GalT-II (Asp-33), respectively) were constructed (Fig. 6A). The culture medium of N2a cells expressing GlcAT-P-sol and prot.A-GalT-I (Ser-43) or -II (Asp-33) was incubated with IgG-Sephar-

Complex of $\beta 4\text{GalT-II}$ and GlcAT-P in HNK-1 Biosynthesis

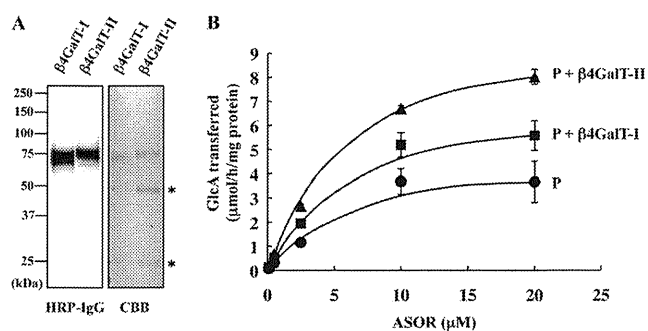


FIGURE 7. Effect of the co-presence of $\beta 4\text{GalT-II}$ on the *in vitro* glucuronyltransferase reaction of GlcAT-P . A, prot.A-GalT-I (Ser-43) ($\beta 4\text{GalT-I}$) or -II (Asp-33) ($\beta 4\text{GalT-II}$) was expressed in COS-1 cells and purified from the culture media. The purified enzymes were subjected to Western blotting with HRP-conjugated rabbit IgG and Coomassie Brilliant Blue (CBB) staining. Asterisks indicate heavy and light chains of immunoglobulin derived from human IgG Sepharose. B, rate of glucuronyltransferase reaction of FLAG-P was measured in the absence of $\beta 4\text{GalTs}$ (P), or in the presence of prot.A-GalT-I (Ser-43) (P + $\beta 4\text{GalT-I}$) or prot.A-GalT-II (Asp-33) (P + $\beta 4\text{GalT-II}$) using different concentrations of ASOR as substrates. All experiments were employed in triplicate, and error bars indicate S.E.

ose beads to pull down the prot.A-tagged enzymes. Subsequent Western blotting was conducted with HRP-conjugated IgG and anti-GlcAT-P pAb (GP2) to detect prot.A-fused enzymes and GlcAT-P, respectively. As shown in Fig. 6B, GlcAT-P-sol was highly co-precipitated with prot.A-GalT-II compared with prot.A-GalT-I, indicating that Golgi luminal domains are enough to form the enzyme complex. To narrow down the binding region of Golgi luminal domains of $\beta 4\text{GalTs}$, we also constructed expression vectors for catalytic domains of $\beta 4\text{GalT-I}$ and -II fused with the signal sequence and protein A (prot.A-GalT-Icat (Leu-129) and prot.A-GalT-IIcat (Ile-91), respectively) and performed pulldown assay as described above. However, neither prot.A-GalT-Icat (Leu-129) nor prot.A-GalT-IIcat (Ile-91) interacts with GlcAT-P-sol (data not shown), suggesting that the deleted stem region are necessary for the specific binding of GlcAT-P and $\beta 4\text{GalT-II}$. Therefore, prot.A-GalT-I (Ser-43) and prot.A-GalT-II (Asp-33) were used for the following kinetic analysis of GlcAT-P.

Kinetic Analysis of GlcAT-P —Next, to investigate whether or not a specific association of $\beta 4\text{GalT-II}$ affects GlcAT-P activity, we examined the dependence of the rate of the glucuronyltransferase reaction on the concentration of ASOR as a glycoprotein acceptor in the presence or absence of $\beta 4\text{GalT-I}$ or $\beta 4\text{GalT-II}$. For this kinetic analysis, we used FLAG-tagged human GlcAT-P (from Thr-58 to the C terminus, FLAG-P) expressed in *E. coli*. The method for expression and purification of FLAG-P had been already established (29). Human GlcAT-P is highly homologous to mouse GlcAT-P, especially 99.3% of amino acids are identical in the region we used (Thr-58 to C terminus). prot.A-GalT-I (Ser-43) and prot.A-GalT-II (Asp-33) were purified from culture media of COS-1 cells that had been transfected with their expression vectors as shown in Fig. 7A. The rate of glucuronyltransferase reaction of FLAG-P in the absence of prot.A-GalTs was compared with that in the presence of prot.A-GalT-I (Ser-43) or prot.A-GalT-II (Asp-33) using different concentrations of ASOR. As shown in Fig. 7B, the rate of FLAG-P reaction was increased depending on the concentration of ASOR and enhanced in the presence of GalT-I

or -II. The data were analyzed by means of Lineweaver-Burk plotting, and the kinetic parameters were then determined (Table 1). Apparent V_{\max} value was increased about 2-fold, and the apparent K_m value was slightly decreased by $\beta 4\text{GalT-II}$. Thus, $\beta 4\text{GalT-II}$ resulted in an approximate 2.5-fold increase in the catalytic efficiency k_{cat}/K_m of FLAG-P. To our surprise, $\beta 4\text{GalT-I}$, which does not associate with GlcAT-P, also enhanced the catalytic efficiency k_{cat}/K_m about 1.7-fold. However, the catalytic efficiency in the presence of $\beta 4\text{GalT-II}$ is still higher than that of $\beta 4\text{GalT-I}$. These results suggest that the enzyme complex of GlcAT-P and $\beta 4\text{GalT-II}$ is indeed capable of facilitating the expression of HNK-1.

Enhanced HNK-1 Biosynthesis by Enzyme Complex in N2a Cells—To determine the effect of the interaction on HNK-1 carbohydrate production in cells, a Western blot analysis was performed with the M6749 mAb. This mAb recognizes nonsulfated HNK-1 carbohydrate (GlcA $\beta 1$ -3Gal $\beta 1$ -4GlcNAc) (38), and N2a cells do not express endogenous GlcAT-P or HNK-1 carbohydrate (Fig. 8A, 1st lane). By employing this antibody, we can examine the level of nonsulfated HNK-1 carbohydrate, which was produced by GlcAT-P (Fig. 8A, 2nd lane). GlcAT-P and $\beta 4\text{GalT-I}$ or -II-myc were co-expressed in N2a cells, and then cell lysates were subjected to SDS-PAGE and Western-blotted with the M6749 mAb, GP2 pAb, and anti-Myc mAb. As shown in Fig. 8A, M6749 immunoreactivity was increased when co-expressed with $\beta 4\text{GalT-I}$ and -II-myc despite the comparable expression of GlcAT-P (compare 2nd lane with 3rd and 4th lanes), probably because of the increased amount of *N*-acetylglucosamine, which can be utilized as an acceptor by GlcAT-P. Intriguingly, however, M6749 immunoreactivity was increased more when GlcAT-P was co-expressed with $\beta 4\text{GalT-II-myc}$ than with $\beta 4\text{GalT-I-myc}$ (Fig. 8A, compare 3rd with 4th lane). To confirm these results, we quantitated two bands (see Fig. 8A, band 1 and 2) by means of densitometric analysis using image analysis software ImageGauge (FujiFilm). As shown in Table 2, co-expression of GlcAT-P and $\beta 4\text{GalT-II-myc}$ caused about 3-fold (see Fig. 8A, bands 1 and 2) increases in M6749 immunoreactivity compared with that of GlcAT-P, and a 2- (band 1) or 1.4-fold (band 2) increase compared with that of GlcAT-P and $\beta 4\text{GalT-I-myc}$. These suggest that $\beta 4\text{GalT-II}$ is better able to promote HNK-1 biosynthesis by associating with GlcAT-P. We carried out a similar analysis with immunoprecipitated NCAM, which is endogenously expressed in N2a cells. As shown in Fig. 8B, the highest expression of the M6749 epitope was observed when GlcAT-P was co-expressed with $\beta 4\text{GalT-II-myc}$. These results suggest that the complex of GlcAT-P and $\beta 4\text{GalT-II}$ contributes to the enhancement of HNK-1 synthesis.

Complex of $\beta 4\text{GalT-II}$ and GlcAT-P in HNK-1 Biosynthesis

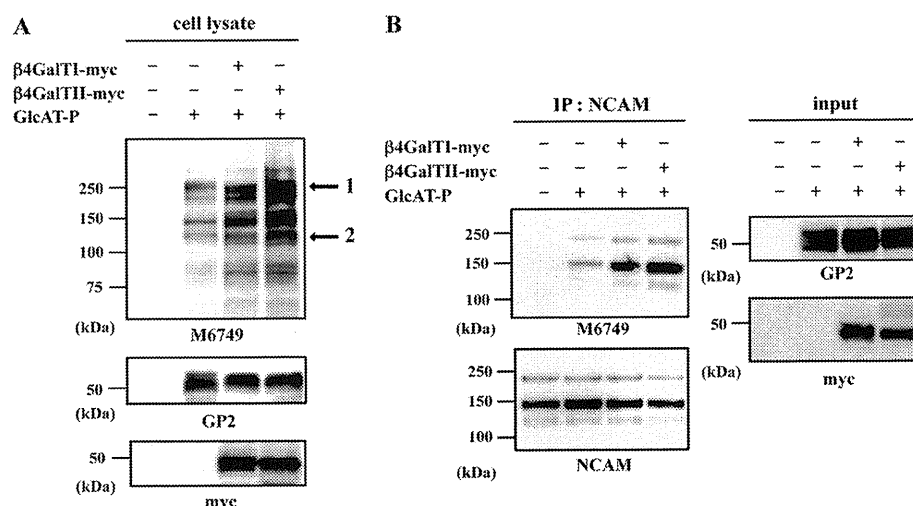


FIGURE 8. Effect of the enzyme complex on HNK-1 expression in N2a cells. *A*, lysates of N2a cells transiently expressing GlcAT-P , $\beta 4\text{GalT-I-myc}$, or $\beta 4\text{GalT-II-myc}$ were subjected to SDS-PAGE and then Western blotted with M6749 mAb, GP2 pAb, or anti-Myc mAb. Arrows indicate bands used for quantification by densitometric analyses. *B*, lysates of N2a cells transiently expressing GlcAT-P and $\beta 4\text{GalT-I-myc}$ or $\beta 4\text{GalT-II-myc}$ were immunoprecipitated (IP) with anti-NCAM mAb and subjected to SDS-PAGE and then Western-blotted with M6749 mAb or anti-NCAM mAb.

TABLE 2
Quantitative analysis of the effect of the enzyme complex

	Mock	GlcAT-P	$\text{GlcAT-P} + \beta 4\text{GalT-I-myc}$	$\text{GlcAT-P} + \beta 4\text{GalT-II-myc}$
Band 1				
Intensity (a.u.) ^a	0	0.48	0.77	1.53
-Fold		1.00	1.60	3.20
Band 2				
Intensity (a.u.)	0	0.21	0.43	0.60
-Fold		1.00	2.03	2.86

^a The immunoreactivity with M6749 mAb was calculated and normalized to GlcAT-P expression and is shown as intensity in arbitrary units (a.u.).

DISCUSSION

The $\beta 4\text{GalT}$ family has seven members, but the biological roles have not been fully understood. We recently reported that $\beta 4\text{GalT-II}$ -deficient mice showed a marked reduction in levels of HNK-1 carbohydrate and impaired spatial memory, and the phenotypes are similar to those of GlcAT-P -deficient mice (19). Moreover, $\beta 4\text{GalT-II}$ is highly expressed in the brain although $\beta 4\text{GalT-I}$ is ubiquitous (39). These findings suggest intrinsic roles *in vivo*, although $\beta 4\text{GalT-I}$ and -II show the highest sequence similarity among $\beta 4\text{GalTs}$. Analyses using these gene-deficient mice revealed that $\beta 4\text{GalT-II}$ is crucial to the production of HNK-1, but the underlying mechanism was not elucidated. In this study, we produced evidence that $\beta 4\text{GalT-II}$ physically associates with GlcAT-P (Figs. 2 and 3) probably through the luminal stem domain of $\beta 4\text{GalT-II}$. Considering the similar domain organizations and molecular sizes of GlcAT-P and $\beta 4\text{GalT-II}$, the stem domain of GlcAT-P may also be involved in this interaction. Because we had revealed that GlcAT-P bound to HNK-1ST through the catalytic region (37), $\beta 4\text{GalT-II}$ seems not to compete with HNK-1ST for the binding to GlcAT-P ; rather, these three enzymes may simultaneously form a large functional complex to synthesize HNK-1 efficiently in living cells. Actually, we revealed that $\beta 4\text{GalT-II}$ is capable of increasing the catalytic efficiency k_{cat}/K_m of the GlcAT-P catalytic reaction using *in vitro* enzyme assay system (Fig. 7). Also in N2a cells, the co-expression of $\beta 4\text{GalT-II}$ and

GlcAT-P enhanced HNK-1 biosynthesis (Fig. 8). These results suggest that HNK-1 expression is regulated by the interaction of these two enzymes.

We found that both $\beta 4\text{GalT-I-}$ and -II- deficient mice showed normal levels of *N*-acetylglucosamine on *N*-glycans, indicating that several $\beta 4\text{GalTs}$ actually contribute to galactosylation in the brain. The specific loss of HNK-1 in $\beta 4\text{GalT-II}$ -deficient mice can be explained in several ways. The present analysis suggests that $\beta 4\text{GalT-II}$ is not the only enzyme for *N*-acetylglucosamine synthesis in HNK-1-expressing cells because *N*-acetylglucosamine is likely expressed at normal levels in $\beta 4\text{GalT-II}$ knock-out mice even on NCAM. Our experiment showed that $\beta 4\text{GalT-II}$ does not specialize in the galactosylation of HNK-1-expressing molecules such as NCAM by recognizing their polypeptide backbones, because the galactosylation of NCAM is unlikely to be impaired in $\beta 4\text{GalT-II}$ knock-out mice. $\beta 4\text{GalT-II}$ might act on a specific *N*-glycosylation site or specific branch of *N*-glycan that is preferentially modified further by GlcAT-P . We demonstrated here that simply the presence of *N*-acetylglucosamine or GlcAT-P is not sufficient for HNK-1 biosynthesis and that both *N*-acetylglucosamines synthesized by $\beta 4\text{GalT-II}$ and GlcAT-P are required. Although $\beta 4\text{GalT-II}$ is involved in HNK-1 biosynthesis, this enzyme is not a chaperone-like molecule for GlcAT-P , because a recombinant GlcAT-P from *E. coli* was fully active without $\beta 4\text{GalT-II}$ *in vitro* (29). Rather, we speculate that $\beta 4\text{GalT-II}$ would be in a specialized complex with GlcAT-P in a specific Golgi compartment to cooperatively catalyze their transfer reactions for HNK-1 synthesis on specific glycoproteins.

To our surprise, $\beta 4\text{GalT-I}$ also had the potential to activate HNK-1 biosynthesis (Fig. 8), even though its effect was weaker than $\beta 4\text{GalT-II}$. This result could be explained by the overproduction of *N*-acetylglucosamine residues by $\beta 4\text{GalT-I}$ overexpression even without enzyme-enzyme interaction. Meanwhile, our *in vitro* analysis also showed that $\beta 4\text{GalT-I}$ weakly activated GlcAT-P catalytic activity (Fig. 7). Although we could not detect the interaction between GlcAT-P and $\beta 4\text{GalT-I}$ in

cell-based co-immunoprecipitation assays, weaker binding was observed in pulldown assays (Fig. 6B). These results suggest that β 4GalT-I could compensate for the loss of HNK-1 biosynthesis in β 4GalT-II-deficient cells if it could be overexpressed. Because HNK-1 expression almost disappeared in the β 4GalT-II-deficient brain, it suggests that the levels of other β 4GalTs in HNK-1-expressing cells may be under the levels that are required for compensation for the loss of β 4GalT-II.

We previously reported that β 4GalT-I- and -II-deficient mice showed the same level of PSA expression as wild-type mice, indicating that the biosynthesis of PSA does not depend on these enzymes (19, 20). Also, we found that PST does not associate with β 4GalT-I or -II (Fig. 4). Regarding the biosynthesis of PSA, another β 4GalT may be associated with polysialyltransferase to specifically synthesize the inner structure of PSA. Alternatively, polysialyltransferase may not distinguish between the inner *N*-acetylglucosamines synthesized by several β 4GalTs. Other β 4GalTs could compensate for the loss of deficiency of a given β 4GalT. Moreover, acidic amino acid residues in the fibronectin type III domain adjacent to the fifth Ig domain of NCAM, which has *N*-glycosylation sites attaching to PSA, were reported to be required for polysialylation (40). PSA biosynthesis would be mainly dependent on the polypeptide backbone of NCAM rather than the enzyme responsible for production of the inner *N*-acetylglucosamine. It is indicated that the biosynthesis of PSA is considerably different from that of HNK-1, despite some common features between these two neural glycans expressed on NCAM.

In recent years, many groups have reported that enzyme complexes of glycosyltransferases have enhanced catalytic activities. Seko and Yamashita (5) showed that a complex of β 3GnT2 and β 3GnT8 produced more poly-*N*-acetylglucosamine. Our previous study demonstrated that GlcAT-P interacts with HNK-1ST, and the interaction enhances the enzymatic activity of HNK-1ST (37). Also, it has been reported that the activities of some glycosyltransferases are regulated through interaction with nonglycosyltransferases. For example, GnT-I activity was inhibited by interaction with GnT-I-IP (GnT-I inhibitory protein), resulting in the expression of high mannose-type *N*-glycans during spermatogenesis (41). T-synthase (C1 β Gal-T) forms a complex with core 1 β 3GalT-specific molecular chaperone, which functions as a specific chaperone. Core 1 β 3GalT-specific molecular chaperone is essential for the T-synthase activity and synthesizing T-antigen (42). Actually, core 1 β 3GalT-specific molecular chaperone is a factor responsible for Tn syndrome, a genetic disease involving a deficiency in T-antigen but no defect in T-synthase (43). In this study, we found that HNK-1 expression is not regulated simply by GlcAT-P but also by the interaction of the enzymes. Supporting this finding, the distribution of GlcAT-P mRNA did not completely match the pattern of HNK-1 expression in the brain. For example, HNK-1 antibody staining showed parasagittal stripes in the molecular layer in the cerebellum (44) because of HNK-1 carbohydrate expression on a limited population of Purkinje cells, whereas GlcAT-P mRNA is likely expressed in most Purkinje cells (45). It would be of interest to compare the distribution of β 4GalT-II mRNA and HNK-1 carbohydrate in the brain. Taken together, to understand the pre-

cise mechanisms of expression and proper functions of glycans, it is important to recognize that many glycosyltransferases form complexes *in vivo*.

HNK-1 carbohydrate has an important role in synaptic plasticity and spine morphogenesis in the nervous system (14, 15). These functions are based on its specific expression on certain carriers such as NCAM and GluR2, which is a subunit of the α -amino-3-hydroxy-5-methylisoxazole propionate-type glutamate receptor. It should be noted that another subunit, GluR1, which forms a complex with GluR2 to make a functional α -amino-3-hydroxy-5-methylisoxazole propionate receptor *in vivo*, is not modified with HNK-1 (46) even if several complex-type *N*-glycans are expressed on GluR1. This indicates that HNK-1 carbohydrate greatly contributes to the specific function of GluR2, but the underlying mechanism of this selective modification is poorly understood. It could be involved in the selective modification to form the complex of β 4GalT-II and GlcAT-P. As well as HNK-1 carbohydrate, many glycans are expressed on specific target proteins, thereby regulating their functions. Thus, it is of great interest to study the mechanisms by which the functions of individual glycosyltransferases are regulated to produce glycoconjugates.

REFERENCES

- Ohtsubo, K., and Marth, J. D. (2006) *Cell* **126**, 855–867
- Lowe, J. B., and Marth, J. D. (2003) *Annu. Rev. Biochem.* **72**, 643–691
- Sugimoto, I., Futakawa, S., Oka, R., Ogawa, K., Marth, J. D., Miyoshi, E., Taniguchi, N., Hashimoto, Y., and Kitazume, S. (2007) *J. Biol. Chem.* **282**, 34896–34903
- Seko, A. (2006) *Trends Glycosci. Glycotechnol.* **18**, 209–230
- Seko, A., and Yamashita, K. (2008) *J. Biol. Chem.* **283**, 33094–33100
- Lee, P. L., Kohler, J. J., and Pfeffer, S. R. (2009) *Glycobiology* **19**, 655–664
- Schwartz, G. A., Jungalwala, F. B., Chou, D. K., Boyer, A. M., and Yamamoto, M. (1987) *Dev. Biol.* **120**, 65–76
- Yoshihara, Y., Oka, S., Watanabe, Y., and Mori, K. (1991) *J. Cell Biol.* **115**, 731–744
- Voshol, H., van Zuylen, C. W., Orberger, G., Vliegthart, J. F., and Schachner, M. (1996) *J. Biol. Chem.* **271**, 22957–22960
- Oka, S., Terayama, K., Kawashima, C., and Kawasaki, T. (1992) *J. Biol. Chem.* **267**, 22711–22714
- Terayama, K., Oka, S., Seiki, T., Miki, Y., Nakamura, A., Kozutsumi, Y., Takio, K., and Kawasaki, T. (1997) *Proc. Natl. Acad. Sci. U.S.A.* **94**, 6093–6098
- Seiki, T., Oka, S., Terayama, K., Imiya, K., and Kawasaki, T. (1999) *Biochem. Biophys. Res. Commun.* **255**, 182–187
- Bakker, H., Friedmann, I., Oka, S., Kawasaki, T., Nifant'ev, N., Schachner, M., and Mantei, N. (1997) *J. Biol. Chem.* **272**, 29942–29946
- Yamamoto, S., Oka, S., Inoue, M., Shimuta, M., Manabe, T., Takahashi, H., Miyamoto, M., Asano, M., Sakagami, J., Sudo, K., Iwakura, Y., Ono, K., and Kawasaki, T. (2002) *J. Biol. Chem.* **277**, 27227–27231
- Morita, I., Kakuda, S., Takeuchi, Y., Kawasaki, T., and Oka, S. (2009) *Neuroscience* **164**, 1685–1694
- Kizuka, Y., Tonoyama, Y., and Oka, S. (2009) *J. Biol. Chem.* **284**, 9247–9256
- Lo, N. W., Shaper, J. H., Pevsner, J., and Shaper, N. L. (1998) *Glycobiology* **8**, 517–526
- Hennet, T. (2002) *Cell. Mol. Life Sci.* **59**, 1081–1095
- Yoshihara, T., Sugihara, K., Kizuka, Y., Oka, S., and Asano, M. (2009) *J. Biol. Chem.* **284**, 12550–12561
- Kido, M., Asano, M., Iwakura, Y., Ichinose, M., Miki, K., and Furukawa, K. (1998) *Biochem. Biophys. Res. Commun.* **245**, 860–864
- Almeida, R., Amado, M., David, L., Levery, S. B., Holmes, E. H., Merckx, G., van Kessel, A. G., Rygaard, E., Hassan, H., Bennett, E., and Clausen, H. (1997) *J. Biol. Chem.* **272**, 31979–31991

Complex of β 4GalT-II and GlcAT-P in HNK-1 Biosynthesis

22. Guo, S., Sato, T., Shirane, K., and Furukawa, K. (2001) *Glycobiology* **11**, 813–820
23. Rutishauser, U. (2008) *Nat. Rev. Neurosci.* **9**, 26–35
24. Mühlenhoff, M., Eckhardt, M., and Gerardy-Schahn, R. (1998) *Curr. Opin. Struct. Biol.* **8**, 558–564
25. Kudo, M., Kitajima, K., Inoue, S., Shiokawa, K., Morris, H. R., Dell, A., and Inoue, Y. (1996) *J. Biol. Chem.* **271**, 32667–32677
26. Asano, M., Furukawa, K., Kido, M., Matsumoto, S., Umesaki, Y., Kochibe, N., and Iwakura, Y. (1997) *EMBO J.* **16**, 1850–1857
27. Kakuda, S., Sato, Y., Tonoyama, Y., Oka, S., and Kawasaki, T. (2005) *Glycobiology* **15**, 203–210
28. Qasba, P. K., Ramakrishnan, B., and Boeggeman, E. (2008) *Curr. Drug Targets* **9**, 292–309
29. Kakuda, S., Oka, S., and Kawasaki, T. (2004) *Protein Expr. Purif.* **35**, 111–119
30. Kruse, J., Mailhammer, R., Wernecke, H., Faissner, A., Sommer, I., Goridis, C., and Schachner, M. (1984) *Nature* **311**, 153–155
31. Nilsson, T., Hoe, M. H., Slusarewicz, P., Rabouille, C., Watson, R., Hunte, F., Watzel, G., Berger, E. G., and Warren, G. (1994) *EMBO J.* **13**, 562–574
32. Giraud, C. G., and Maccioni, H. J. (2003) *Mol. Biol. Cell* **14**, 3753–3766
33. Eckhardt, M., Mühlenhoff, M., Bethe, A., Koopman, J., Frosch, M., and Gerardy-Schahn, R. (1995) *Nature* **373**, 715–718
34. Kojima, N., Yoshida, Y., and Tsuji, S. (1995) *FEBS Lett.* **373**, 119–122
35. Nakayama, J., and Fukuda, M. (1996) *J. Biol. Chem.* **271**, 1829–1832
36. Breton, C., Mucha, J., and Jeanneau, C. (2001) *Biochimie* **83**, 713–718
37. Kizuka, Y., Matsui, T., Takematsu, H., Kozutsumi, Y., Kawasaki, T., and Oka, S. (2006) *J. Biol. Chem.* **281**, 13644–13651
38. Tagawa, H., Kizuka, Y., Ikeda, T., Itoh, S., Kawasaki, N., Kurihara, H., Onozato, M. L., Tojo, A., Sakai, T., Kawasaki, T., and Oka, S. (2005) *J. Biol. Chem.* **280**, 23876–23883
39. Nakamura, N., Yamakawa, N., Sato, T., Tojo, H., Tachi, C., and Furukawa, K. (2001) *J. Neurochem.* **76**, 29–38
40. Mendiratta, S. S., Sekulic, N., Lavie, A., and Colley, K. J. (2005) *J. Biol. Chem.* **280**, 32340–32348
41. Huang, H. H., and Stanley, P. (2010) *J. Cell Biol.* **190**, 893–910
42. Ju, T., and Cummings, R. D. (2002) *Proc. Natl. Acad. Sci. U.S.A.* **99**, 16613–16618
43. Ju, T., and Cummings, R. D. (2005) *Nature* **437**, 1252
44. Marzban, H., Sillitoe, R. V., Hoy, M., Chung, S. H., Rafuse, V. F., and Hawkes, R. (2004) *J. Neurocytol.* **33**, 117–130
45. Inoue, M., Kato, K., Matsuhashi, H., Kizuka, Y., Kawasaki, T., and Oka, S. (2007) *Brain Res.* **1179**, 1–15
46. Morita, I., Kakuda, S., Takeuchi, Y., Itoh, S., Kawasaki, N., Kizuka, Y., Kawasaki, T., and Oka, S. (2009) *J. Biol. Chem.* **284**, 30209–30217

Chondroitin 4-O-sulfotransferase-1 regulates the chain length of chondroitin sulfate in co-operation with chondroitin N-acetylgalactosaminyltransferase-2

Tomomi IZUMIKAWA¹, Yuka OKUURA¹, Toshiyasu KOIKE, Naoki SAKODA and Hiroshi KITAGAWA²

Department of Biochemistry, Kobe Pharmaceutical University, Higashinada-ku, Kobe 658-8558, Japan

Previously, we demonstrated that *sog9* cells, a murine L cell mutant, are deficient in the expression of C4ST (chondroitin 4-O-sulfotransferase)-1 and that they synthesize fewer and shorter CS (chondroitin sulfate) chains. These results suggested that C4ST-1 regulates not only 4-O-sulfation of CS, but also the length and amount of CS chains; however, the mechanism remains unclear. In the present study, we have demonstrated that C4ST-1 regulates the chain length and amount of CS in co-operation with ChGn-2 (chondroitin N-acetylgalactosaminyltransferase 2). Overexpression of ChGn-2 increased the length and amount of CS chains in L cells, but not in *sog9* mutant cells. Knockdown of ChGn-2 resulted in a decrease in the amount of CS in L cells in a manner proportional to ChGn-2 expression levels, whereas

the introduction of mutated C4ST-1 or ChGn-2 lacking enzyme activity failed to increase the amount of CS. Furthermore, the non-reducing terminal 4-O-sulfation of N-acetylgalactosamine residues facilitated the elongation of CS chains by chondroitin polymerase consisting of chondroitin synthase-1 and chondroitin-polymerizing factor. Overall, these results suggest that the chain length of CS is regulated by C4ST-1 and ChGn-2 and that the enzymatic activities of these proteins play a critical role in CS elongation.

Key words: chondroitin sulfate, glycosaminoglycan, glycosyltransferase, proteoglycan, sulfotransferase.

INTRODUCTION

CS (chondroitin sulfate) is a class of GAG (glycosaminoglycan) that is widely distributed on the surface of cells and within the extracellular matrix. CS is covalently linked to specific serine residues of core proteins and occurs as CS PGs (proteoglycans). CS moieties vary considerably in the size and number of GAG chains per core protein and in the position and degree of sulfation; therefore these highly variable moieties are able to store a massive amount of information and exert a variety of biological functions [1,2]. CS and characteristic CS chains exert their specific functions in a tissue- and cell-type-specific manner, suggesting that sulfation and polymerization of CS chains are strictly regulated. A previous study suggested that CS elongation is associated with increased binding of atherogenic lipids and atherosclerosis [3]. Moreover, deficiency in SLC35D1 (solute carrier 35D1), which encodes an endoplasmic reticulum nucleotide–sugar transporter, caused shortening of CS chains and led to skeletal dysplasias [4]. Therefore an understanding of the CS chain elongation mechanism is essential for elucidating multiple pathogenic mechanisms.

Multiple glycosyltransferases and sulfotransferases are responsible for the biosynthesis of CS [5] (Figure 1). The synthesis of the linkage tetrasaccharide sequence, the so-called GAG–protein linkage region (GlcA β 1-3Gal β 1-3Gal β 1-4Xyl β 1-O-Ser), is initiated by the addition of a xylose (Xyl) residue to a specific serine (Ser) residue in the core protein, followed by the sequential transfer of galactose (Gal) residues,

and completed by the addition of the glucuronic acid (GlcA) residue [5]. Following completion of the synthesis of the linkage tetrasaccharide sequence, polymerization of repeating disaccharide units occurs by the alternate transfer of GlcA and GalNAc (N-acetylgalactosamine) [5]. Then, a number of sulfotransferases modify the chondroitin backbone with sulfate at positions 4 and 6 of the GalNAc residues and position 2 of the GlcA residues, resulting in structural diversity of CS moieties [6].

To date, six homologous glycosyltransferases, ChSy (chondroitin synthase)-1, ChSy-2, ChSy-3, ChPF (chondroitin-polymerizing factor), and ChGn (chondroitin N-acetylgalactosamine transferase)-1 and -2, all of which are probably responsible for CS biosynthesis, have been cloned by us and others [7–14]. We have demonstrated chondroitin polymerization with alternating GalNAc and GlcA residues when any two of ChSy-1, ChSy-2, ChSy-3 and ChPF were co-expressed [8–10] (Figure 1). ChGn-1 and -2 are thought to catalyse chain initiation and elongation, exhibiting activities of GalNAcT (β 1,4-N-acetylgalactosaminyltransferase)-I and -II [11–14] (Figure 1). In addition, seven sulfotransferases involved in the sulfation of CS have been cloned to date [6]. Four sulfotransferases that catalyse sulfation of position 4 of the GalNAc residue have been cloned. C4ST (chondroitin 4-O-sulfotransferase)-1, -2 and -3 are responsible for the sulfation of position 4 of GalNAc residues in CS, whereas D4ST (dermatan 4-O-sulfotransferase)-1 catalyses the transfer of a sulfate residue to GalNAc residues next to IdoA (iduronic acid) in DS (dermatan sulfate) [15–19] (Figure 1). C6ST-1 (chondroitin 6-O-sulfotransferase-1) transfers

Abbreviations used: C4ST, chondroitin 4-O-sulfotransferase; C6ST-1, chondroitin 6-O-sulfotransferase-1; ChGn, chondroitin N-acetylgalactosaminyltransferase; ChPF, chondroitin-polymerizing factor; ChSy, chondroitin synthase; CS, chondroitin sulfate; D4ST, dermatan 4-O-sulfotransferase; GAG, glycosaminoglycan; GalNAc4S-6ST, N-acetylgalactosamine 4-sulfate 6-O-sulfotransferase; GalNAcT, β 1,4-N-acetylgalactosaminyltransferase; GAPDH, glyceraldehyde-3-phosphate dehydrogenase; PAPS, adenosine 3'-phosphate 5'-phosphosulfate; PDGF, platelet-derived growth factor; PG, proteoglycan; RT, reverse transcription; shRNA, short hairpin RNA; TGF β , transforming growth factor β .

¹ These authors contributed equally to this work.

² To whom correspondence should be addressed (email kitagawa@kobepharma-u.ac.jp).

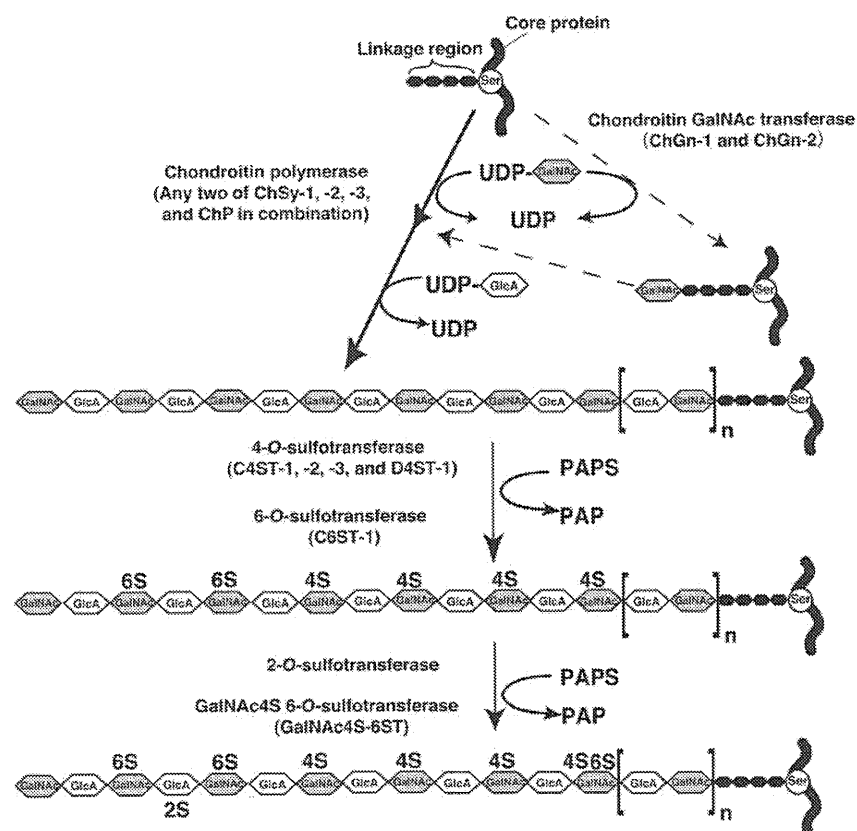


Figure 1 Biosynthesis of CS

CS is synthesized as PGs on specific serine residues in the GAG-protein linkage region, $\text{GlcA}\beta 1\text{-3Gal}\beta 1\text{-3Gal}\beta 1\text{-4Xyl}\beta 1\text{-O-Ser}$. Following completion of the synthesis of the linkage tetrasaccharide sequence, the transfer of a single GalNAc residue to the tetrasaccharide linkage region by any two of ChSy-1, ChSy-2, ChSy-3 and ChPF (continuous arrow), or by ChGn-1 and -2 (broken arrow) initiates the assembly of CS. Polymerization then occurs through alternate addition of GlcA and GalNAc by any two of ChSy-1, ChSy-2, ChSy-3 and ChPF. Following synthesis of the backbone of CS, modifications of the precursor CS chains are conducted by various sulfotransferases. The first modifications, 4-O-sulfation or 6-O-sulfation of GalNAc residues, are catalysed by 4-O-sulfotransferases (C4ST-1, -2 and -3, and D4ST-1) or 6-O-sulfotransferase (C6ST-1) respectively. Thereafter, 2-O-sulfation of GlcA or 6-O-sulfation of GalNAc(4S) residues are catalysed by uronyl 2-O-sulfotransferase or GalNAc4S-6ST respectively.

sulfate to position 6 of the GalNAc residue [20,21]. Uronyl 2-O-sulfotransferase catalyses the 2-O-sulfation of GlcA and IdoA. GalNAc4S-6ST (N-acetylgalactosamine 4-sulfate 6-O-sulfotransferase) transfers a sulfate residue to position 6 of GalNAc(4S) formed by C4ST [22] (Figure 1).

Previously, we demonstrated that *sog9* mutant cells were deficient in the expression of C4ST-1 and synthesized shorter CS chains with low 4-O-sulfation levels and that overexpression of C4ST-2 or D4ST-1 in *sog9* cells did not lead to an increase in the chain length or amount of CS [23]. In addition, C4ST-1-deficient mice showed a 90% decrease in GalNAc(4S) structures and a severe reduction in the amount of CS [24]. These results suggested that C4ST-1 regulates CS 4-O-sulfation, chain length and amount; moreover, other C4ST/D4ST family members, including C4ST-2 and D4ST-1, does not compensate for the loss of C4ST-1. Therefore the 4-O-sulfation of CS chains by C4ST-1 may facilitate the elongation of CS chains; however, the C4ST-1 mechanism remains elusive. We hypothesized that 4-O-sulfation of non-reducing terminal GalNAc formed by ChGn-1 or -2 markedly enhances the elongation of CS chains by chondroitin polymerases. In the present paper, we report that C4ST-1 co-operates with ChGn-2 in CS chain elongation.

EXPERIMENTAL

Materials

UDP-[U- ^{14}C]GlcA (285.2 mCi/mmol) and UDP-[^3H]GalNAc (10 Ci/mmol) were purchased from NEN Life Science Products. Unlabelled UDP-GlcA and UDP-GalNAc were obtained from Sigma. ^{35}S -labelled PAPS (adenosine 3'-phosphate 5'-phosphosulfate) (1.69 mCi/mmol) was purchased from PerkinElmer Life Sciences. Chondroitin (a chemically desulfated derivative of whale cartilage CS-A), *Proteus vulgaris* chondroitinase ABC (EC 4.2.2.4), and *Arthrobacter aureescens* chondroitinase ACII were purchased from Seikagaku. Even-numbered regular chondro-oligosaccharides, $(4\text{GlcA}\beta 1\text{-3GalNAc}\beta 1\text{-})_2$, $[4\text{GlcA}\beta 1\text{-3GalNAc}(4\text{S})\beta 1\text{-}]_2$ and Oligo-2 (see Table 1), were prepared by hyaluronidase digestion of chondroitin or whale cartilage CS-A followed by gel filtration on a Bio-Gel P-10 column (1.6 cm \times 95 cm) and HPLC on an amine-bound silica column as described in [25]. Odd-numbered chondro-oligosaccharides, Oligo-1, Oligo-3 and Oligo-4 (see Table 1), were prepared by partially digesting chondroitin with chondroitinase ABC followed by mercuric acetate treatment [26], and purified by gel filtration on a Bio-Gel P-10 column

Table 1 Structure of oligosaccharides used as acceptors

Oligosaccharide	Structure
Oligo-1	GalNAc β 1-(4GlcA β 1-3GalNAc β 1-) ₂
Oligo-2	(4GlcA β 1-3GalNAc β 1-) ₃
Oligo-3	GalNAc β 1-(4GlcA β 1-3GalNAc β 1-) ₅
Oligo-4	GalNAc β 1-(4GlcA β 1-3GalNAc β 1-) ₇
Oligo-5	GalNAc(4S) β 1-4GlcA β 1-3GalNAc(4S) β 1-4GlcA β 1-3GalNAc(4S)
Oligo-6	GalNAc β 1-4GlcA β 1-3GalNAc(4S) β 1-4GlcA β 1-3GalNAc(4S)

(1.6 cm \times 95 cm) followed by HPLC on an amine-bound silica column as described previously [25]. A sulfated pentasaccharide, Oligo-5 (see Table 1), used as an acceptor, was isolated by HPLC after partial chondroitinase ABC digestion of whale cartilage CS-A followed by mercuric acetate treatment. The resulting pentasaccharide was then structurally characterized using enzymatic digestion. A partially sulfated pentasaccharide, Oligo-6 (see Table 1), used as an acceptor, was synthesized by ChGn-2 from [4GlcA β 1-3GalNAc(4S) β 1-]₂ prepared above. It was purified by HPLC and structurally characterized enzymatically. Superdex™ Peptide HR10/30, Superdex™ Peptide 75 and Superdex™ 200 10/300 GL columns were obtained from GE Healthcare. Mouse L fibroblasts and their mutant derivatives, sog9 cells, were kindly provided by Dr Frank Tufaro (Allera Health Products, St. Petersburg, FL, U.S.A.). Sog9-C4ST-1-1 (high expression) and sog9-C4ST-1-5 (low expression) cells were isolated previously [23].

Establishment of an expression vector for ChGn-1 and ChGn-2, and preparation of cells that stably express transfected ChGn-1 and ChGn-2

The cDNA fragment encoding *ChGn-1* was amplified by RT (reverse transcription) using total RNA from G361 human melanoma cells (A.T.C.C. CRL-1424) as a template and a 5'-primer (5'-CGGGATCCTTGGACGCGATGGCTGATTC-3') and a 3'-primer (5'-CGGGATCCTTGGACGCGATGGCTGATTC-3') each containing a BamHI site. The cDNA fragment encoding *ChGn-2* was amplified by RT using total RNA from G361 human melanoma cells as a template and a 5'-primer (5'-CGCGGATCCTTGTAGGCAAATACACATTAATAAG-3') and a 3'-primer (5'-CGCGGATCCTTGTAGGCAAATACACATTAATAAG-3') each containing a BamHI site. PCR was carried out with *KOD-Plus* DNA polymerase (TOYOBO) for 30 cycles at 94°C for 30 s, 53°C for 42 s and 68°C for 180 s in 5% (v/v) DMSO. The PCR fragments were subcloned into the BamHI site of the pCMV expression vector (Invitrogen). The fidelity of the plasmid constructs (pCMV-ChGn-1 and pCMV-ChGn-2) was confirmed by DNA sequencing. The expression plasmid (6.7 μ g) was transfected into L and sog9 cells on 100-mm-diameter plates using FuGENE® 6 (Roche) according to the manufacturer's instructions. Transfectants were cultured in the presence of 300 μ g/ml G418. Transfected colonies were picked up and propagated for experiments.

ChGn-2 silencing in L cells was performed using MISSION shRNA (short hairpin RNA) (Sigma). The shRNA plasmid (6.7 μ g) was transfected into L cells on 100-mm-diameter plates using FuGENE® 6 according to the manufacturer's instructions. Transfectants were cultured in the presence of 0.4 mg/ml puromycin. Resultant colonies were then picked up and propagated for experiments.

Site-directed mutagenesis

A two-stage PCR mutagenesis method was used to construct separate ChGn-2 and C4ST-1 mutants. Two separate PCRs were performed to generate two overlapping gene fragments using the full-length form of *ChGn-2* or *C4ST-1* cDNA as a template. In the first PCR, the sense 5'-primer described above and the antisense internal mutagenic primer listed below was used: ChGn-2 D184A 5'-AAATAGATATCAACAGCACAGAAAAACATC-3' (the mutated nucleotides are underlined and in bold). In the second round of PCR, the sense internal mutagenic primer (complementary to the antisense internal mutagenic primer) and the antisense 3'-primer described above were used. In the case of C4ST-1, the sense 5'-primer (5'-GAAGATCTAGGACAAAGCCATGAAGCCGGC-3') and the antisense internal mutagenic primer C4ST-1 R586A 5'-CTCGAAGGGTTCCCGCCACGAACAGGAA-3' (the mutated nucleotides are underlined and in bold) were used. In the second round of PCR, the sense internal mutagenic primer (complementary to the antisense internal mutagenic primer) and the antisense 3'-primer (5'-ATAACCCAGTCTCCATAGAATTCTTTTGA-3') were used. These two PCR products were gel-purified and then used as a template for a third PCR containing the sense 5'-primer and the antisense 3'-primer described above. The final PCR fragment was subcloned into the BamHI site or BamHI/EcoRI site of the pCMV expression vector respectively (Invitrogen). The fidelity of the plasmid constructs (pCMV-ChGn-2 D367A and pCMV-C4ST-1 R186A) was confirmed by DNA sequencing.

Quantitative real-time RT-PCR

Total RNA was extracted from L and sog9 cells using TRIzol® reagent (Invitrogen). The cDNA was synthesized from ~1 μ g of total RNA using Moloney murine leukaemia virus reverse transcriptase (Promega) and an oligo(dT)₂₀-M4 adaptor primer (TaKaRa). The primer sequences used were as follows: ChGn-1, forward primer 5'-AGAAGAA-TAAATGAAGTCAAAGGAATAC-3' and reverse primer 5'-GAAGTAGATGTCCACATCACAG-3'; and ChGn-2, forward primer 5'-CCTAGAATCTGTCACCAGT-3' and reverse primer 5'-GTTAAGGAATTCGGCTGAGAAATA-3'; and GAPDH (glyceraldehyde-3-phosphate dehydrogenase), forward primer 5'-CATCTGAGGGCCCACTG-3' and reverse primer 5'-GAGGCCATGTAGGCCATGA-3'. Quantitative real-time RT-PCR was performed using a FastStart DNA Master plus SYBR Green I (Roche) in a LightCycler ST300 (Roche). The expression levels of *ChGn-1* or *ChGn-2* mRNA were normalized to that of the GAPDH transcript.

Derivatization of GAGs from L and sog9 cells using a fluorophore, 2-aminobenzamide

GAGs from L and sog9 cells were prepared as described previously [23,27]. The purified GAG fraction was digested with chondroitinase ABC, and the digests were then derivatized with 2-aminobenzamide and analysed by HPLC as described previously [23].

Gel-filtration chromatography of GAGs

To determine the chain length of GAGs, the purified GAG fraction was subjected to reductive β -elimination using NaBH₄/NaOH, and then analysed by gel-filtration chromatography on a Superdex™ 200 column (10 mm \times 300 mm) eluted with 0.2 M NH₄HCO₃ at a flow rate of 0.4 ml/min. Fractions were collected at 3-min intervals, freeze-dried and digested with chondroitinase

ABC. The digests were derivatized with 2-aminobenzamide and then analysed by HPLC on an amine-bound PA-03 column [28].

Polymerization assay and identification of polymerization reaction products

The ChSy-1 and ChPF expression plasmids (3.0 µg each) were co-transfected into COS-1 cells on 100-mm plates using FuGENE® 6 as described previously [10]. At 2 days after transfection, 1 ml of the culture medium was collected and incubated with 10 µl of IgG–Sepharose (GE Healthcare) for 1 h at 4°C. The beads recovered by centrifugation were washed with, and resuspended in, the assay buffer and then tested for N-acetylgalactosaminyltransferase activity, as described previously [29]. The oligosaccharides used are listed in Table 1. Polymerization reactions using Oligo-1, Oligo-2, Oligo-5 and Oligo-6 as acceptors were co-incubated in reaction mixtures containing the following constituents in a total volume of 20 µl: 1 nmol of Oligo-1, -2, -5 or -6, 0.25 mM UDP-GalNAc, 0.25 mM UDP-[¹⁴C]GlcA (3 × 10⁵ d.p.m.), 100 mM Mes (pH 6.5), 10 mM MnCl₂ and 10 µl of the resuspended beads. The mixtures were incubated at 37°C overnight. The products of the polymerization reactions were isolated by gel filtration on a Superdex™ 75 column with 0.25 M NH₄HCO₃/0.7% propan-1-ol as the eluent.

Expression of the soluble forms of recombinant C4ST-1 and C4ST-2 and identification of reaction products

Each expression plasmid (6.0 µg) was transfected into COS-1 cells on 100-mm-diameter plates using FuGENE® 6 according to the manufacturer's instructions and as described previously [19]. At 2 days after transfection, 1 ml of the culture medium was collected and incubated with 10 µl of IgG–Sepharose for 1 h at 4°C. The beads recovered by centrifugation were washed with and then resuspended in the assay buffer, and tested for sulfotransferase activity. Assays for sulfotransferase were described previously [19] with slight modifications. Briefly, the standard reaction mixture (30 µl) contained 10 µl of resuspended beads, 50 mM imidazole/HCl (pH 6.8), 2 mM dithiothreitol, 10 µM [³⁵S]PAPS (3 × 10⁵ d.p.m.), and 1 nmol of Oligo-3 or Oligo-4 as an acceptor substrate respectively. The reaction mixtures were incubated at 37°C overnight and gel-filtered using a syringe column packed with Sephadex G-25 (superfine) [30]. The radioactive fractions containing the enzyme reaction products were pooled and desiccated. The isolated reaction product was digested with chondroitinase AC-II. The products of enzymatic digestion were analysed using the Superdex™ peptide column with 0.25 M NH₄HCO₃/0.7% propan-1-ol as the eluent.

RESULTS

Introduction of ChGn-1 or ChGn-2 into sog9 and L cells

To examine whether ChGn-1 or/and ChGn-2 collaborates with C4ST-1 to regulate the length of CS chains, overexpression of ChGn-1 or ChGn-2 in L and sog9 cells was carried out. A pCMV-Script expression vector harbouring the open reading frame of human ChGn-1 or ChGn-2 was transfected into sog9 or L cells, and the neomycin analogue G418 was used to select transfected cells. Each of the resultant transfected colonies was picked and propagated for experiments, and the expression of ChGn-1 or ChGn-2 in the cells was measured by quantitative real-time RT–PCR. As shown in Tables 2 and 3, the composition of the disaccharides and the amount of CS isolated from the stable clones, designated L-ChGn-1, L-ChGn-2, sog9-ChGn-1 and sog9-ChGn-2 cells, were determined by HPLC. Whereas

Table 2 Disaccharide composition of CS in control and transfected L cells

Values in (a) are means ± S.E.M. of three determinations, expressed in pmol of disaccharide/mg of dried cell homogenate, with mol% in parentheses. N.D., not detected (<0.01 pmol/mg). In (b), relative amounts of the ChGn-1 and ChGn-2 (including, if any, the mutant) transcripts were quantified by quantitative real-time RT–PCR. Data were normalized to GAPDH mRNA levels.

Disaccharide	(a)										(b)		
	L-mock	L-ChGn-1-1	L-ChGn-1-2	L-ChGn-2-1	L-ChGn-2-2	L-shRNA ChGn-2-1	L-shRNA ChGn-2-2	L-ChGn-2 D367A-1	L-ChGn-2 D367A-2	L-ChGn-2 D367A-1	L-ChGn-2 D367A-2	Relative expression of ChGn-1	Relative expression of ChGn-2
ΔDi-OS	22 ± 3 (6)	38 ± 9 (10)	38 ± 5 (10)	33 ± 5 (7)	32 ± 4 (7)	42 ± 2 (13)	23 ± 3 (9)	20 ± 1 (7)	25 ± 1 (8)	20 ± 1 (7)	25 ± 1 (8)	1.0	1.0
ΔDi-6S	3 ± 1 (1)	2 ± 2 (1)	2 ± 1 (1)	12 ± 11 (2)	7 ± 6 (1)	25 ± 3 (8)	12 ± 3 (4)	3 ± 2 (1)	4 ± 0 (1)	3 ± 2 (1)	4 ± 0 (1)	0.9	1.6
ΔDi-4S	283 ± 6 (80)	309 ± 38 (83)	299 ± 20 (81)	403 ± 26 (81)	398 ± 23 (82)	235 ± 5 (71)	207 ± 9 (79)	238 ± 23 (83)	258 ± 12 (81)	238 ± 23 (83)	258 ± 12 (81)	2.4	1.6
ΔDi-diSo	N.D.	N.D.	N.D.	N.D.	N.D.	N.D.	N.D.	N.D.	N.D.	N.D.	N.D.	0.9	0.2
ΔDi-diSe	47 ± 3 (13)	22 ± 19 (6)	30 ± 10 (8)	49 ± 27 (10)	48 ± 16 (10)	28 ± 2 (8)	20 ± 1 (8)	27 ± 6 (9)	31 ± 4 (10)	27 ± 6 (9)	31 ± 4 (10)	0.5	0.2
Total	355 ± 13	371 ± 17	369 ± 21	497 ± 30	485 ± 29	330 ± 12	262 ± 16	288 ± 27	318 ± 16	288 ± 27	318 ± 16	1.0	1.0
	L-mock	L-ChGn-1-1	L-ChGn-1-2	L-ChGn-2-1	L-ChGn-2-2	L-shRNA ChGn-2-1	L-shRNA ChGn-2-2	L-ChGn-2 D367A-1	L-ChGn-2 D367A-2	L-ChGn-2 D367A-1	L-ChGn-2 D367A-2	0.9	2.4

Table 3 Disaccharide composition of CS in control and transfected sog9 cells

Values in (a) are means \pm S.E.M. of three determinations, expressed in pmol of disaccharide/mg of dried cell homogenate, with mol% in parentheses. N.D., not detected (<0.01 pmol/mg). In (b), relative amounts of the *ChGn-1*, *ChGn-2* and *C4ST-1* (including, if any, the mutant) transcripts were quantified by quantitative real-time RT-PCR. Data were normalized to *GAPDH* mRNA levels. —, not determined.

(a)	Sog9-mock	Sog9-ChGn-1-1	Sog9-ChGn-1-2	Sog9-ChGn-2-1	Sog9-ChGn-2-2	Sog9-C4ST-1-1	Sog9-C4ST-1-5	Sog9-C4ST-1 R186A-1	Sog9-C4ST-1 R186A-2
Δ Di-OS	63 \pm 3 (55)	56 \pm 13 (33)	58 \pm 10 (41)	68 \pm 12 (61)	67 \pm 12 (63)	48 \pm 1 (16)	91 \pm 1 (50)	67 \pm 10 (58)	66 \pm 7 (56)
Δ Di-6S	10 \pm 2 (8)	15 \pm 4 (9)	9 \pm 4 (6)	10 \pm 7 (9)	8 \pm 4 (7)	11 \pm 0 (3)	13 \pm 2 (7)	9 \pm 1 (8)	11 \pm 3 (9)
Δ Di-4S	40 \pm 7 (35)	94 \pm 15 (56)	71 \pm 10 (51)	32 \pm 14 (29)	31 \pm 10 (29)	220 \pm 6 (73)	73 \pm 7 (40)	38 \pm 5 (33)	40 \pm 8 (34)
Δ Di-diS ₀	N.D.	N.D.	N.D.	N.D.	N.D.	N.D.	N.D.	N.D.	N.D.
Δ Di-diS ₀	2 \pm 1 (2)	3 \pm 3 (2)	2 \pm 2 (2)	1 \pm 2 (1)	1 \pm 1 (1)	25 \pm 2 (8)	5 \pm 2 (3)	1 \pm 1 (1)	1 \pm 1 (1)
Total	115 \pm 15	168 \pm 20	140 \pm 19	111 \pm 14	107 \pm 19	304 \pm 8	182 \pm 9	115 \pm 14	118 \pm 14
(b)	Sog9-mock	Sog9-ChGn-1-1	Sog9-ChGn-1-2	Sog9-ChGn-2-1	Sog9-ChGn-2-2	Sog9-C4ST-1-1	Sog9-C4ST-1-5	Sog9-C4ST-1 R186A-1	Sog9-C4ST-1 R186A-2
Relative expression of <i>ChGn-1</i>	1.0	3.2	1.3	1.0	1.0	1.2	1.1	1.0	1.0
Relative expression of <i>ChGn-2</i>	1.0	1.0	1.0	5.0	4.5	1.0	1.1	1.0	1.0
Relative expression of <i>C4ST-1</i>	—	—	—	—	—	0.7	0.4	1.0	0.5

the disaccharide compositions in L-ChGn-1 and L-ChGn-2 cells were similar to those in control L cells, the amount of CS was greater in L-ChGn-1 and L-ChGn-2 cells than in the controls (Table 2). Although the proportion of Δ Di-4S [Δ HexA α 1-3GalNAc(4S)] units and the total amount of CS was higher in sog9-ChGn-1 than in controls, the proportion of the Δ Di-4S subunits and the amount of CS in sog9-ChGn-2 cells was similar to that in control sog9 cells (Table 3). These results indicated that overexpression of ChGn-2 increased the amounts of CS in L cells, but not in sog9 cells, and that ChGn-2 can regulate the amount of CS only in the presence of C4ST-1.

Prompted by these observations, we next examined whether knockdown of ChGn-2 decreases the amount of CS in L cells. The efficiency of gene silencing was determined by quantitative real-time RT-PCR. As shown in Table 2, transfection of *ChGn-2* shRNA (L-shRNA ChGn-2-1 and L-shRNA ChGn-2-2 cells: two different shRNAs directed against *ChGn-2* were used) resulted in a 50 or 80 % knockdown of *ChGn-2* mRNA and a 7 or 26 % decrease in the amount of CS when compared with control L cells. These findings indicated that knockdown of *ChGn-2* decreased the amounts of CS in L cells, corresponding to the expression levels of ChGn-2 (Table 2). Therefore ChGn-2 can regulate the amount of CS, and the amount of CS is proportional to ChGn-2 expression levels.

Involvement of ChGn-2 in CS chain elongation

We next compared the length of CS chains obtained from L-ChGn-2-1, L-shRNA ChGn-2-2, sog9-ChGn-2-1, and mock-transfected L and sog9 cells. Gel-filtration analysis using a SuperdexTM 200 column revealed that CS chains in L-ChGn-2-1 cells were much longer than in control L cells, whereas CS chains in L-shRNA ChGn-2-2 cells were markedly shorter than in control L cells (Figure 2A). In contrast, CS chains in sog9-ChGn-2-1 cells were shorter than in mock-transfected cells (Figure 2B). These results indicated that the expression of ChGn-2 in the presence of C4ST-1 resulted in longer and more abundant CS chains. In addition, in the absence of C4ST-1, ChGn-2 did not regulate CS chain length. Notably, the length of CS chains in L-shRNA ChGn-2-2 cells was comparable with that in sog9 cells (Figures 2A and 2B), suggesting that ChGn-2 and C4ST-1 have non-redundant functions in the chain elongation of CS and that the two enzymes co-operate to elongate CS chains.

Contribution of enzyme activity of ChGn-2 or C4ST-1 in CS biosynthesis

To determine whether N-acetylgalactosaminyltransferase activity of ChGn-2 contributed to chain elongation, we constructed a ChGn-2 mutant that lacked enzymatic activity. On the basis of the sequence alignment of ChSy family members, ChGn-2 has only one putative DXD motif, DVD (Asp³⁶⁷-Val-Asp³⁶⁹), and DXD motifs are responsible for UDP-sugar binding in many glycosyltransferases [31]. It was therefore expected that the ChGn-2 D367A (AVD) mutant would not have N-acetylgalactosaminyltransferase activity. To confirm the expression and activity of ChGn-2 D367A, the soluble mutant was generated by replacing the first 36 amino acids of ChGn-2 D367A with a cleavable insulin signal sequence and the Protein A IgG-binding domain, as described previously [14]. The soluble mutant protein was expressed and evaluated for N-acetylgalactosaminyltransferase activity; as expected, no such activity was detected. We then investigated whether overexpression of ChGn-2 D367A increased the amount of CS

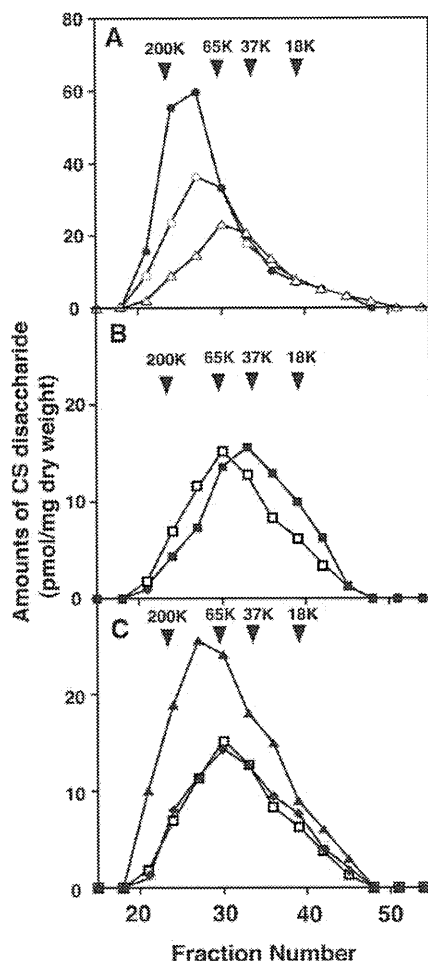


Figure 2 Analysis of the length of CS chains from L, L-ChGn-2-1, L-shRNA ChGn-2-2, sog9, sog9-ChGn-2-1, sog9-C4ST-1-1 and sog9-C4ST-1 R186A-1 cells by gel-filtration chromatography

The purified CS fraction was subjected to reductive β -elimination using $\text{NaBH}_4/\text{NaOH}$ and then analysed by gel-filtration chromatography on a column (10 mm \times 300 mm) of SuperdexTM 200. The digests of individual fractions obtained with chondroitinase ABC were derivatized with 2-aminobenzamide and then analysed by HPLC. The amounts of the 2-aminobenzamide derivatives of unsaturated disaccharides were calculated on the basis of fluorescence intensity. (A) Samples from L-ChGn-2-1 (\bullet), L-shRNA ChGn-2-2 (Δ) and mock-transfected L cells (\circ) are shown. (B) Samples from sog9-ChGn-2-1 (\blacksquare) and mock-transfected sog9 cells (\square) are shown. (C) Samples from sog9-C4ST-1-1 (\blacktriangle), sog9-C4ST-1 R186A-1 (\blacklozenge) and mock-transfected sog9 cells (\square) are shown. Numbered arrowheads 200K, 65K, 37K and 18K indicate the eluted position of 200, 65, 37 and 18 kDa saccharides derived from size-defined commercial dextran respectively. Results are from one series of independent experiments representative of three, where the three series of experiments gave essentially identical results.

in L cells. As shown in Table 2, the amount and disaccharide composition of CS isolated from each of the representative stable clones were similar to control L cells. These results indicated that the N-acetylgalactosaminyltransferase activity of ChGn-2 played an essential role in increasing CS levels.

Next, to verify that the sulfotransferase activity of C4ST-1 contributed to CS chain elongation, the C4ST-1 mutant, which lacks sulfotransferase activity, was overexpressed in sog9 cells. The mutated form of C4ST-1 (C4ST-1 R186A), which fails to bind PAPS, was described previously [32]. The disaccharide composition and the amount of CS in C4ST-1 R186A cells

were analysed by HPLC (Table 3). The amount of CS and the disaccharide composition in sog9-C4ST-1 R186A cells were similar to those in control sog9 cells (Table 3).

We next compared the length of CS chains obtained from sog9-C4ST-1-1 [23], sog9-C4ST-1 R186A-1 and mock-transfected sog9 cells. Gel-filtration analysis using a SuperdexTM 200 column revealed that CS chains in sog9-C4ST-1-1 cells were longer than those in sog9-C4ST-1 R186A-1 or control sog9 cells (Figure 2C). The mean molecular masses were 101 (sog9-C4ST-1-1), 78 (sog9-C4ST-1 R186A-1) and 79 kDa (control sog9 cells) respectively (Figure 2C). Notably, the length of CS chains in sog9-C4ST-1 R186A-1 was comparable with that in sog9 cells (Figure 2C). These findings indicated that CS levels were not rescued by introduction of the mutated C4ST-1 R186A; therefore the enzymatic activity of both ChGn-2 and C4ST-1 was necessary to regulate the amount and chain length of CS.

Involvement of non-reducing terminal GalNAc(4S) structure in chondroitin polymerization

We predicted that the non-reducing terminal 4-O-sulfation of GalNAc residues that are newly synthesized by C4ST-1 and ChGn-2 may facilitate the elongation of CS chains by the chondroitin polymerases that synthesize the CS backbone. Previously, we demonstrated that chondroitin polymerization occurred when any two of ChSy-1, ChSy-2, ChSy-3 and ChPF were co-expressed [8–10] (see Figure 1). Hence, polymerization activity was measured using Oligo-1, -2, -5 or -6 as acceptor substrates and ChSy-1 co-expressed with ChPF as the initial enzyme source. Each reaction product obtained with Oligo-1, -2, -5 or -6 was analysed by gel-filtration chromatography using a SuperdexTM 75 column, as shown in Figure 3(A). The chondroitin chains synthesized on Oligo-5 were much longer than those synthesized on Oligo-1, -2 or -6. In contrast, no polymerization was induced on these acceptor oligosaccharides when co-expressed ChSy-1 and ChSy-2, ChSy-1 and ChSy-3, ChSy-2 and ChSy-3, ChSy-2 and ChPF, or ChSy-3 and ChPF were used (see Supplementary Figure S1 and Supplementary Table S1 at <http://www.BiochemJ.org/bj/434/bj4340321add.htm>). Interestingly, although *ChSy-1* and *ChPF* mRNA were expressed in both L and sog9 cells, *ChSy-2* and *ChSy-3* mRNA were hardly expressed in these cell lines (see Supplementary Figure S2 at <http://www.BiochemJ.org/bj/434/bj4340321add.htm>). These results indicated that chondroitin polymerization by the ChSy-1/ChPF enzyme complex was facilitated by the non-reducing terminal GalNAc(4S) structure (Figure 3B).

Substrate specificity of C4ST-1 for the non-reducing terminal GalNAc

Previously, it has been reported that C4ST-1 catalyses the transfer of sulfate from PAPS to position 4 of the internal GalNAc residue of chondroitin [18,19]; however, it is not clear whether C4ST-1 is also responsible for transferring the sulfate to position 4 of the non-reducing terminal GalNAc residue. Hence, we examined the sulfotransferase activity of C4ST-1 at a non-reducing terminal GalNAc residue. However, C4ST-1 did not use the trisaccharide GalNAc β 1-4GlcA β 1-3GalNAc as a substrate. Then, the sulfotransferase activity was determined using longer oligosaccharides such as Oligo-3 or -4 as the acceptor substrates and [³⁵S]PAPS as the donor substrate. The ³⁵S-labelled products were digested exhaustively with chondroitinase AC-II, which cleaves the β 1-4-N-acetylgalactosaminidic linkage; two radioactive peaks were detected at the GalNAc-4-O-SO₄ and Δ Di-4S positions

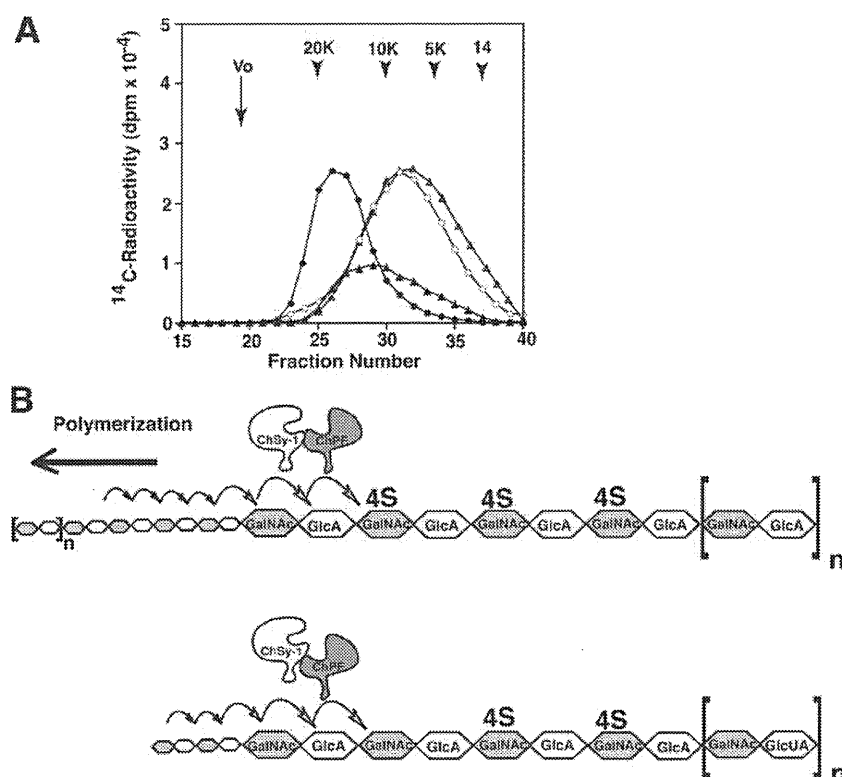


Figure 3 Comparison of the sizes of the chondroitin polymerization reaction products obtained using various acceptors containing different non-reducing terminal structures

(A) Oligo-1 (Δ), Oligo-2 (\circ), Oligo-5 (\bullet) and Oligo-6 (\blacktriangle) were each tested as an acceptor of polymerization reactions as described previously [10]. ^{14}C -labelled polymerization reaction products were isolated by gel filtration on a SuperdexTM 75 column with 0.25 M NH_4HCO_3 /0.7% propan-1-ol as the eluent. Numbered arrowheads 20K, 10K, 5K and 14 indicate the eluted position of 20, 10 and 5 kDa saccharides and tetradecasaccharides derived from chondroitin respectively. The total volume was at fraction ~ 60 (not shown). (B) Schematic representation of the results obtained in (A). Further elongation of CS chains by the enzyme complex of ChSy-1 and ChPF was facilitated by the non-reducing terminal GalNAc(4S) structure, but not the non-reducing terminal GalNAc structure.

in 1:10 (Figure 4A for Oligo-3, \circ) or 1:6 molar ratios (Figure 4B for Oligo-4, \circ) respectively. In sharp contrast, C4ST-2 transferred the sulfate only to the internal GalNAc residues (Figures 4A and 4B, \bullet). These results indicated that C4ST-1 transferred the sulfate from PAPS to the non-reducing terminal GalNAc residue and to the internal GalNAc residues (Figure 4C). Thus 4-O-sulfation of the non-reducing terminal structure of CS chains by C4ST-1 facilitated the elongation of CS chains by chondroitin polymerases that synthesize the CS backbone.

DISCUSSION

Previously, we demonstrated that sog9 cells, a murine L cell mutant, were deficient in C4ST-1 and synthesized shorter CS chains [23]. The transfection of C4ST-1 into sog9 cells resulted in a recovery in the amount of CS and an increase in the length of the CS chains; moreover, the expression level of C4ST-1 correlated well with the recovery of 4-O-sulfated CS levels [23]. In addition, C4ST-1-deficient mice showed a 90% decrease in GalNAc(4S) structures as well as a severe reduction in the amount of CS [24]. Although these results suggested that C4ST-1 regulates not only 4-O-sulfation of CS, but also the amounts and length of CS

chains, the C4ST-1 mechanism was not clear because C4ST-1 is only responsible for the sulfation of the 4-O-position of GalNAc residues in CS chains. In the present study, we showed that C4ST-1 co-operates with ChGn-2 in chain elongation of CS moieties (Figure 5). Overexpression of ChGn-2 increased the amount and chain length of CS in L cells, but not in sog9 cells (Tables 2 and 3). Knockdown of ChGn-2 decreased the amount of CS in L cells in a manner relative to ChGn-2 expression levels (Table 2). Additionally, the amount of CS was not increased by the introduction of mutated C4ST-1 or ChGn-2, both of which lacked enzyme activity. Furthermore, the non-reducing terminal 4-O-sulfation of GalNAc residues facilitated the elongation of CS chains through chondroitin polymerase consisting of ChSy-1 and ChPF (Figures 3 and 5). Notably, the similar tissue distribution profiles of ChGn-2 and C4ST-1 suggest further that these enzymes co-operate in the synthesis of CS moieties [13–15,18].

In a previous study, *in vitro* chondroitin polymerization was demonstrated when α -thrombomodulin, which contains a truncated GAG–protein linkage region tetrasaccharide sequence, was used as an acceptor with the co-expression of any two of ChSy-1, ChSy-2, ChSy-3 and ChPF as enzyme sources [8–10]. The findings indicate that ChGn-1 and ChGn-2 [11–14], which harbour both GalNAcT-I and -II activities, are dispensable for chondroitin polymerization at the linkage

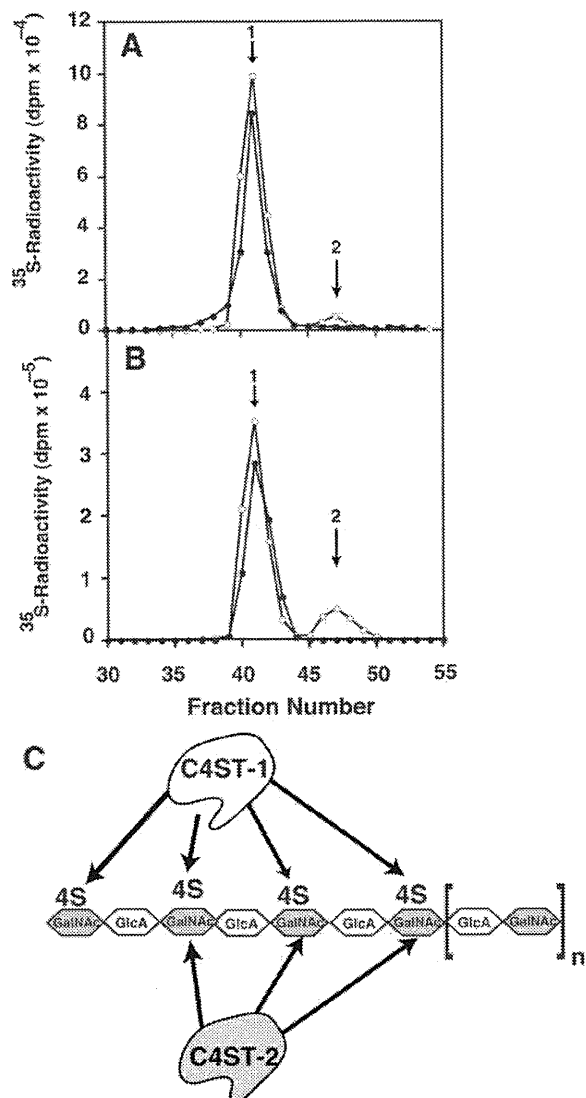


Figure 4 Identification of ^{35}S -labelled sulfotransferase reaction products prepared using C4ST-1 or C4ST-2 as the enzyme source

^{35}S -labelled sulfotransferase reaction products, prepared using C4ST-1 or C4ST-2 with Oligo-3 (A) or Oligo-4 (B) as the sulfate acceptor respectively were digested with chondroitinase AC-II. The chondroitinase AC-II digest derived from reaction products using C4ST-1 (○) or C4ST-2 (●) was isolated by gel filtration on a Superdex™ Peptide column with 0.25 M NH_4HCO_3 /0.7% propan-1-ol as the eluent. The numbered arrowheads indicate the elution positions of: 1, $\Delta\text{Di-4S}$; and 2, GalNAc-4- SO_4 . (C) Schematic representation of the results obtained in (A) and (B). The arrows indicate the potential sulfation site in the schematic repeating disaccharide sequence of CS catalysed by C4ST-1 and C4ST-2. C4ST-1 transferred the sulfate from PAPS to the non-reducing terminal GalNAc residue as well as the internal GalNAc residues. In sharp contrast, C4ST-2 transferred the sulfate only to the internal GalNAc residues.

region tetrasaccharide sequence. However, the present study demonstrated that overexpression of ChGn-2 increased CS amounts and chain lengths, but overexpression of a mutated ChGn-2 lacking enzymatic activity failed to increase the amount of CS in L cells. Thus ChGn-2 was involved in the chain-elongation mechanism of CS, and its enzymatic function played an important role in this chain elongation.

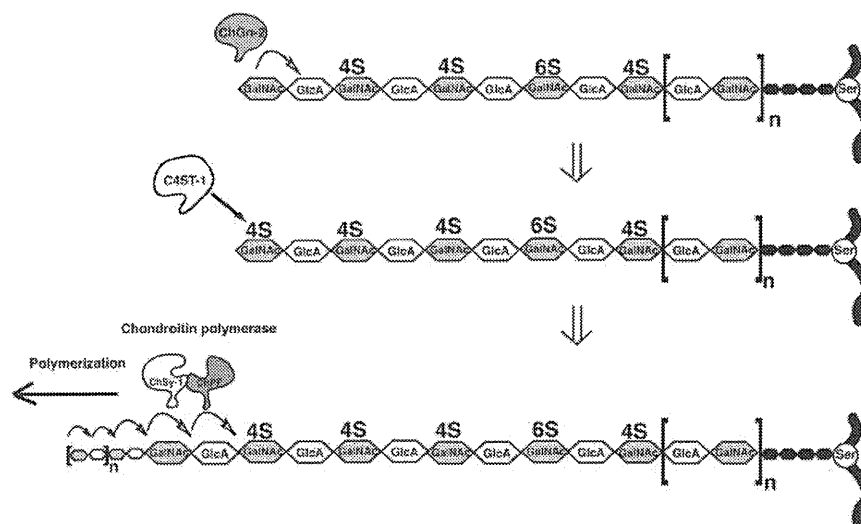
In contrast, overexpression of ChGn-1 in *sog9* cells increased the total amount of CS and the proportion of $\Delta\text{Di-4S}$ units compared with that in controls and in *sog9* cells overexpressing ChGn-2 (Table 3). These results suggested that the function of ChGn-1 was different from that of ChGn-2. Previously, it was revealed that C4ST-1 mRNA is not expressed in *sog9* cells, whereas C4ST-2 and D4ST-1 mRNA are expressed [23]. Thus ChGn-1 regulation of the amount of CS through its cooperation with C4ST-2 and/or D4ST-1 was expected. Comparative analysis of ChGn-1 [33] and ChGn-2-knockout mice would provide further insight into the distinct functions of these genes.

In *Caenorhabditis elegans* and *Drosophila melanogaster*, CS is synthesized as non-sulfated chondroitin and 4-O-sulfated CS respectively [34,35]. Additionally, in *C. elegans*, there is a single orthologue for each of ChSy and ChPF, but none for ChGn-1 or -2, despite the existence of chondroitin in the nematode [36]. In fact, the ChSy and ChPF orthologues are sufficient to synthesize chondroitin, and the system for chondroitin biosynthesis in *C. elegans* seems to be simpler than those in *D. melanogaster* and mammals [37]. On the other hand, there is a single orthologue for each of ChSy, ChPF and ChGn in *D. melanogaster*. Our group showed previously that the mean chain length of chondroitin in *C. elegans* is short (~ 40 kDa) and that of CS in *D. melanogaster* is ~ 70 kDa [34,35]. These results, together with those of the present study, strongly suggested that the GalNAc-4-O-sulfation of CS chains by C4ST and ChGn facilitated the elongation of CS chains by a chondroitin polymerase (e.g. the ChSy–ChPF complex) which is involved in synthesizing the CS backbone. Hence, we predicted that the diverse size of CS chains per core protein is strictly regulated not only by chondroitin polymerase, but also by CS sulfotransferases and N-acetylgalactosaminyltransferases. In addition, we suggest that these mechanisms are highly conserved through evolution.

Earlier studies have indicated that the sulfation of GAG chains ordinarily occurs in conjunction with polymerization at a single Golgi site and that there appears to be close interrelationships between sulfation and polymer elongation/termination [38]. In fact, our previous findings revealed that specific sulfate groups have either stimulatory or inhibitory effects on GalNAc transfer, and, consequently, sulfation reactions indeed play important roles in chain elongation and termination [29,39]. In addition, we reveal in the present study that the non-reducing terminal 4-O-sulfation of GalNAc residues synthesized by C4ST-1 and ChGn-2 facilitated the elongation of CS chains through chondroitin polymerase consisting of ChSy-1 and ChPF (Figures 3 and 5). In this regard, it should be noted that there is a progressive decrease in 4-sulfation to 4,6-disulfation of GalNAc residues on the non-reducing terminal residues of CS in human cartilage during development [40]. Moreover, the CS chains on aggrecan isolated from human cartilage become shorter with age [40]; therefore we suggest that the prior specific sulfation patterns in growing CS chains profoundly affected chain elongation and termination.

Previously, it was demonstrated that human lung fibroblasts treated with TGF β (transforming growth factor β) alone or in combination with EGF (epidermal growth factor) and PDGF (platelet-derived growth factor) increased the production of CS PG and the activity of C4ST-1 [41]. In addition, it was reported that TGF β or PDGF treatment of arterial smooth muscle cells results in the elongation of CS chains [3,42,43]. CS elongation is reported to be associated with increased binding of atherogenic lipids and atherosclerosis progression [3]. We demonstrated that C4ST-1 regulated the chain length and amount of CS in cooperation with ChGn-2; therefore these mitogens might promote the elongation of CS by controlling the expression of relevant

A GlcA on the non-reducing termini



B GalNAc on the non-reducing termini

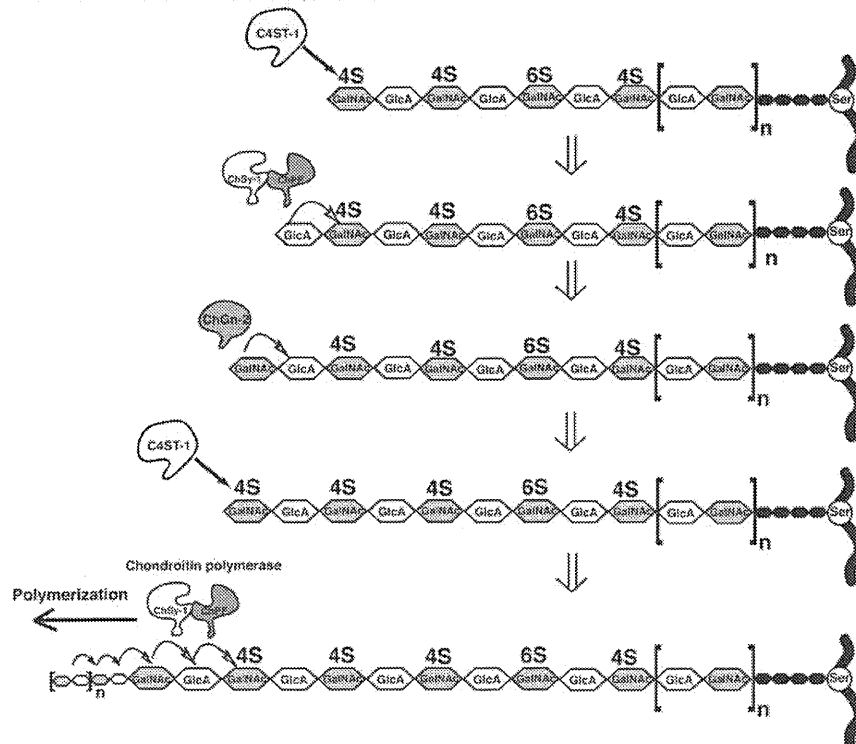


Figure 5 Models of CS chain elongation by ChGn-2 and C4ST-1

(A) In the case of GlcA on the termini, the transfer of GalNAc to the disaccharide-repeating region by ChGn-2 is a trigger of further CS chain elongation. 4-O-sulfation of the non-reducing terminal GalNAc residue then takes place by C4ST-1. Finally, the non-reducing terminal 4-O-sulfation of GalNAc residues facilitates the elongation of CS chains through chondroitin polymerase consisting of ChSy-1 and ChPF. (B) In the case of GalNAc on the termini, the action of C4ST-1 is followed by the transfer of GlcA by the enzyme complex of ChSy-1 and ChPF. Next, ChGn-2 transfers GalNAc to the non-reducing terminal GlcA and 4-O-sulfation of the non-reducing terminal GalNAc residue takes place by C4ST-1. Finally, the non-reducing terminal 4-O-sulfation of GalNAc residues facilitates the elongation of CS chains through chondroitin polymerase consisting of ChSy-1 and ChPF.

enzymes, such as C4ST-1 and ChGn-2. Thus understanding the mechanisms that regulate the expression of C4ST-1 and ChGn-2 during atherosclerosis progression may lead to the identification of potential therapeutic targets for intervention in the pathological process of atherosclerosis.

AUTHOR CONTRIBUTION

Tomomi Izumikawa, Yuka Okuura, Toshiyasu Koike and Naoki Sakoda performed the research; Hiroshi Kitagawa designed the research; Tomomi Izumikawa, Yuka Okuura and Hiroshi Kitagawa analysed the data; and Tomomi Izumikawa and Hiroshi Kitagawa wrote the paper.

ACKNOWLEDGEMENTS

We are especially grateful to Professor Frank Tufaro for kindly providing the sog9 cells. We also thank Dr Toru Uyama for valuable discussion, and Yuuki Tamaki for technical assistance.

FUNDING

This work was supported in part by the Science Research Promotion Fund of the Japan Private School Promotion Foundation, Health Sciences Research Grant on Psychiatric and Neurological Diseases and Mental Health [grant number H21-012] from the Ministry of Health, Labour and Welfare of Japan, and Grants-in-aid for Scientific Research-B [grant number 21390025 (to H.K.)] from the Ministry of Education, Culture, Sports, Science and Technology (MEXT), Japan.

REFERENCES

- Perrimon, N. and Bernfield, M. (2000) Specificities of heparan sulphate proteoglycans in developmental processes. *Nature* **404**, 725–728
- Sugahara, K. and Kitagawa, H. (2000) Recent advances in the study of the biosynthesis and functions of sulfated glycosaminoglycans. *Curr. Opin. Struct. Biol.* **10**, 518–527
- Little, P. J., Tannock, L., Olin, K. L., Chait, A. and Wight, T. N. (2002) Proteoglycans synthesized by arterial smooth muscle cells in the presence of transforming growth factor- β 1 exhibit increased binding to LDLs. *Arterioscler. Thromb. Vasc. Biol.* **22**, 55–60
- Hiraoka, S., Furuichi, T., Nishimura, G., Shibata, S., Yanagishita, M., Rimoim, D. L., Superti-Furga, A., Nikkels, P. G., Ogawa, M., Katsuyama, K. et al. (2007) Nucleotide-sugar transporter SLC35D1 is critical to chondroitin sulfate synthesis in cartilage and skeletal development in mouse and human. *Nat. Med.* **13**, 1363–1367
- Silbert, J. E. and Sugumaran, G. (2002) Biosynthesis of chondroitin/dermatan sulfate. *IUBMB Life* **54**, 177–186
- Kusche-Gullberg, M. and Kjellén, L. (2003) Sulfotransferases in glycosaminoglycan biosynthesis. *Curr. Opin. Struct. Biol.* **13**, 605–611
- Kitagawa, H., Uyama, T. and Sugahara, K. (2001) Molecular cloning and expression of a human chondroitin synthase. *J. Biol. Chem.* **276**, 38721–38726
- Izumikawa, T., Uyama, T., Okuura, Y., Sugahara, K. and Kitagawa, H. (2007) Involvement of chondroitin sulfate synthase-3 (chondroitin synthase-2) in chondroitin polymerization through its interaction with chondroitin synthase-1 or chondroitin polymerizing factor. *Biochem. J.* **403**, 545–552
- Izumikawa, T., Koike, T., Shiozawa, S., Sugahara, K., Tamura, J. and Kitagawa, H. (2008) Identification of chondroitin sulfate glucuronyltransferase as chondroitin synthase-3 involved in chondroitin polymerization: chondroitin polymerization is achieved by multiple enzyme complexes consisting of chondroitin synthase family members. *J. Biol. Chem.* **283**, 11396–11406
- Kitagawa, H., Izumikawa, T., Uyama, T. and Sugahara, K. (2003) Molecular cloning of a chondroitin polymerizing factor that cooperates with chondroitin synthase for chondroitin polymerization. *J. Biol. Chem.* **278**, 23666–23671
- Uyama, T., Kitagawa, H., Tamura, J. and Sugahara, K. (2002) Molecular cloning and expression of human chondroitin *N*-acetylgalactosaminyltransferase: the key enzyme for chain initiation and elongation of chondroitin/dermatan sulfate on the protein linkage region tetrasaccharide shared by heparin/heparan sulfate. *J. Biol. Chem.* **277**, 8841–8846
- Gotoh, M., Sato, T., Akashima, T., Iwasaki, H., Kameyama, A., Mochizuki, H., Yada, T., Inaba, N., Zhang, Y., Kikuchi, N. et al. (2002) Enzymatic synthesis of chondroitin with a novel chondroitin sulfate *N*-acetylgalactosaminyltransferase that transfers *N*-acetylgalactosamine to glucuronic acid in initiation and elongation of chondroitin sulfate synthesis. *J. Biol. Chem.* **277**, 38189–38196
- Sato, T., Gotoh, M., Kiyohara, K., Akashima, T., Iwasaki, H., Kameyama, A., Mochizuki, H., Yada, T., Inaba, N., Togayachi, A. et al. (2003) Differential roles of two *N*-acetylgalactosaminyltransferases, CSGalNAcT-1, and a novel enzyme, CSGalNAcT-2. Initiation and elongation in synthesis of chondroitin sulfate. *J. Biol. Chem.* **278**, 3063–3071
- Uyama, T., Kitagawa, H., Tanaka, J., Tamura, J., Ogawa, T. and Sugahara, K. (2003) Molecular cloning and expression of a second chondroitin *N*-acetylgalactosaminyltransferase involved in the initiation and elongation of chondroitin/dermatan sulfate. *J. Biol. Chem.* **278**, 3072–3078
- Hiraoka, N., Nakagawa, H., Ong, E., Akama, T. O., Fukuda, M. N. and Fukuda, M. (2000) Molecular cloning and expression of two distinct human chondroitin 4-*O*-sulfotransferases that belong to the HNK-1 sulfotransferase gene family. *J. Biol. Chem.* **275**, 20188–20196
- Kang, H.-G., Evers, M. R., Xia, G., Baenziger, J. U. and Schachner, M. (2002) Molecular cloning and characterization of chondroitin-4-*O*-sulfotransferase-3: a novel member of the HNK-1 family of sulfotransferases. *J. Biol. Chem.* **277**, 34766–34772
- Evers, M. R., Xia, G., Kang, H.-G., Schachner, M. and Baenziger, J. U. (2001) Molecular cloning and characterization of a dermatan-specific *N*-acetylgalactosamine 4-*O*-sulfotransferase. *J. Biol. Chem.* **276**, 36344–36354
- Yamauchi, S., Mita, S., Matsubara, T., Fukuta, M., Habuchi, H., Kimata, K. and Habuchi, O. (2000) Molecular cloning and expression of chondroitin 4-sulfotransferase. *J. Biol. Chem.* **275**, 8975–8981
- Mikami, T., Mizumoto, S., Kago, N., Kitagawa, H. and Sugahara, K. (2003) Specificities of three distinct human chondroitin/dermatan *N*-acetylgalactosamine 4-*O*-sulfotransferases demonstrated using partially desulfated dermatan sulfate as an acceptor: implication of differential roles in dermatan sulfate biosynthesis. *J. Biol. Chem.* **278**, 36115–36127
- Fukuta, M., Uchimura, K., Nakashima, K., Kato, M., Kimata, K., Shinomura, T. and Habuchi, O. (1995) Molecular cloning and expression of chick chondrocyte chondroitin 6-sulfotransferase. *J. Biol. Chem.* **270**, 18575–18580
- Tsutsumi, K., Shimakawa, H., Kitagawa, H. and Sugahara, K. (1998) Functional expression and genomic structure of human chondroitin 6-sulfotransferase. *FEBS Lett.* **441**, 235–241
- Ohtake, S., Ito, Y., Fukuta, M. and Habuchi, O. (2001) Functional expression and genomic structure of human chondroitin 6-sulfotransferase. *J. Biol. Chem.* **276**, 43894–43900
- Uyama, T., Ishida, M., Izumikawa, T., Trybala, E., Tufaro, F., Bergström, T., Sugahara, K. and Kitagawa, H. (2006) Chondroitin 4-*O*-sulfotransferase-1 regulates E disaccharide expression of chondroitin sulfate required for herpes simplex virus infectivity. *J. Biol. Chem.* **281**, 38668–38674
- Klüppel, M., Wight, T. N., Chan, C., Hinek, A. and Wrana, J. L. (2005) Maintenance of chondroitin sulfation balance by chondroitin-4-sulfotransferase 1 is required for chondrocyte development and growth factor signaling during cartilage morphogenesis. *Development* **132**, 3989–4003
- Sugahara, K., Okumura, Y. and Yamashina, I. (1989) The Engelbreth—Holm—Swarm mouse tumor produces undersulfated heparan sulfate and oversulfated galactosaminoglycans. *Biochem. Biophys. Res. Commun.* **162**, 189–197
- Ludwigs, U., Elgavish, A., Esko, J. D., Meezan, E. and Rodén, L. (1987) Reaction of unsaturated uronic acid residues with mercuric salts: cleavage of the hyaluronic acid disaccharide 2-acetamido-2-deoxy-3-*O*- β -D-glucuro-4-ene-pyranosyluronic acid)-D-glucose. *Biochem. J.* **245**, 795–804
- Nadanaka, S., Ishida, M., Ikegami, M. and Kitagawa, H. (2008) Chondroitin 4-*O*-sulfotransferase-1 modulates Wnt-3a signaling through control of E disaccharide expression of chondroitin sulfate. *J. Biol. Chem.* **283**, 27333–27343
- Koike, T., Izumikawa, T., Tamura, J. and Kitagawa, H. (2009) FAM20B is a kinase that phosphorylates xylose in the glycosaminoglycan—protein linkage region. *Biochem. J.* **421**, 157–162
- Kitagawa, H., Tsutsumi, K., Ujikawa, M., Goto, F., Tamura, J., Neumann, K. W., Ogawa, T. and Sugahara, K. (1997) Regulation of chondroitin sulfate biosynthesis by specific sulfation: acceptor specificity of serum β -GalNAc transferase revealed by structurally defined oligosaccharides. *Glycobiology* **7**, 531–537
- Kitagawa, H., Tsuchida, K., Ujikawa, M. and Sugahara, K. (1995) Detection and characterization of UDP-GalNAc: chondroitin *N*-acetylgalactosaminyltransferase in bovine serum using a simple assay method. *J. Biochem. (Tokyo)* **117**, 1083–1087
- Wiggins, C. A. and Munri, S. (1998) Activity of the yeast MNN1 α -1,3-mannosyltransferase requires a motif conserved in many other families of glycosyltransferases. *Proc. Natl. Acad. Sci. U.S.A.* **95**, 7945–7950
- Wang, H., Katagiri, Y., McCann, T. E., Unsworth, E., Goldsmith, P., Yu, Z. X., Tan, F., Santiago, L., Mills, E. M., Wang, Y. et al. (2008) Chondroitin-4-sulfation negatively regulates axonal guidance and growth. *J. Cell Sci.* **121**, 3083–3091
- Watanabe, Y., Takeuchi, K., Higa-Onaga, S., Tsujita, M., Abe, M., Natsume, R., Li, M., Furuichi, T., Saeki, M., Izumikawa, T. et al. (2010) Chondroitin sulfate *N*-acetylgalactosaminyltransferase-1 is required for normal cartilage development. *Biochem. J.* **432**, 47–55
- Yamada, S., Van Die, I., Van den Eijnden, D. H., Yokota, A., Kitagawa, H. and Sugahara, K. (1999) Demonstration of glycosaminoglycans in *Caenorhabditis elegans*. *FEBS Lett.* **459**, 327–331
- Yamada, S., Okada, Y., Ueno, M., Iwata, S., Deepa, S. S., Nishimura, S., Fujita, M., Van Die, I., Hirabayashi, Y. and Sugahara, K. (2002) Determination of the glycosaminoglycan—protein linkage region oligosaccharide structures of proteoglycans from *Drosophila melanogaster* and *Caenorhabditis elegans*. *J. Biol. Chem.* **277**, 31877–31886
- Mizuguchi, S., Uyama, T., Kitagawa, H., Nomura, K. H., Dejima, K., Gengyo-Ando, K., Mitani, S., Kohara, Y., Sugahara, K. and Nomura, K. (2003) Chondroitin proteoglycans are involved in cell division of *Caenorhabditis elegans*. *Nature* **423**, 443–448
- Izumikawa, T., Kitagawa, H., Mizuguchi, S., Nomura, K. H., Nomura, K., Tamura, J., Gengyo-Angyo, K., Mitani, S. and Sugahara, K. (2004) Nematode chondroitin polymerizing factor showing cell-/organ-specific expression is indispensable for chondroitin synthesis and embryonic cell division. *J. Biol. Chem.* **279**, 53755–53761
- Silbert, J. E. and Sugumaran, G. (1995) Intracellular membranes in the synthesis, transport, and metabolism of proteoglycans. *Biochim. Biophys. Acta* **1241**, 371–384
- Kitagawa, H., Ujikawa, M., Tsutsumi, K., Tamura, J., Neumann, K. W., Ogawa, T. and Sugahara, K. (1997) Characterization of serum β -glucuronyltransferase involved in chondroitin sulfate biosynthesis. *Glycobiology* **7**, 905–911

-
- 40 Plaas, A. H., Wong-Palms, S., Roughley, P. J., Midura, R. J. and Hascall, V. C. (1997) Chemical and immunological assay of the nonreducing terminal residues of chondroitin sulfate from human aggrecan. *J. Biol. Chem.* **272**, 20603–20610
- 41 Tiedemann, K., Olander, B., Eklund, E., Todorova, L., Bengtsson, M., Maccarana, M., Westergren-Thorsson, G. and Malmström, A. (2005) Regulation of the chondroitin/dermatan fine structure by transforming growth factor- β 1 through effects on polymer-modifying enzymes. *Glycobiology* **15**, 1277–1285
- 42 Schönherr, E., Järveläinen, H. T., Sandell, L. J. and Wight, T. N. (1991) Effects of platelet-derived growth factor and transforming growth factor- β 1 on the synthesis of a large versican-like chondroitin sulfate proteoglycan by arterial smooth muscle cells. *J. Biol. Chem.* **266**, 17640–17647
- 43 Schönherr, E., Järveläinen, H. T., Kinsella, M. G., Sandell, L. J. and Wight, T. N. (1993) Platelet-derived growth factor and transforming growth factor- β 1 differentially affect the synthesis of biglycan and decorin by monkey arterial smooth muscle cells. *Arterioscler. Thromb.* **13**, 1026–1036
-

Received 10 September 2010/29 November 2010; accepted 8 December 2010

Published as BJ Immediate Publication 8 December 2010, doi:10.1042/BJ20101456

SUPPLEMENTARY ONLINE DATA

Chondroitin 4-O-sulfotransferase-1 regulates the chain length of chondroitin sulfate in co-operation with chondroitin N-acetylgalactosaminyltransferase-2

Tomomi IZUMIKAWA¹, Yuka OKUURA¹, Toshiyasu KOIKE, Naoki SAKODA and Hiroshi KITAGAWA²

Department of Biochemistry, Kobe Pharmaceutical University, Higashinada-ku, Kobe 658-8558, Japan

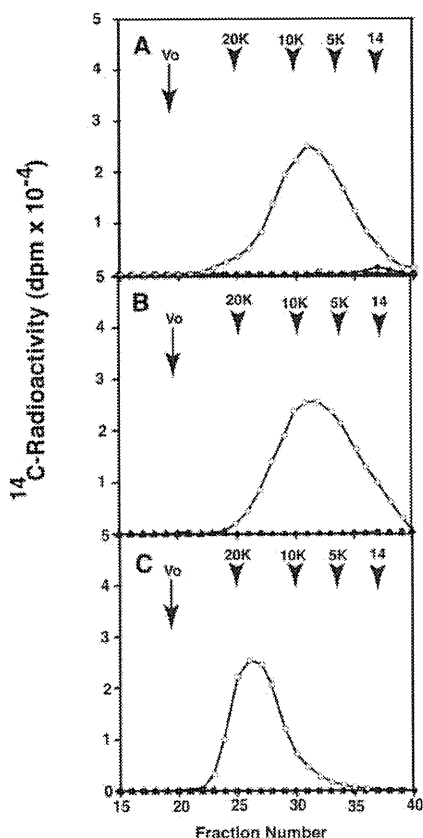


Figure S1 Comparison of chondroitin-polymerizing activity using various combinations of ChSy-1, ChSy-2, ChSy-3 and ChPF

Combinations of ChSy-1 and ChPF (○), ChSy-1 and ChSy-2 (▲), ChSy-1 and ChSy-3 (●), ChSy-2 and ChSy-3 (□), ChSy-2 and ChPF (■), or ChSy-3 and ChPF (△) were tested as an enzyme source for polymerization reactions using the non-sulfated hexasaccharide Oligo-2 (A), the non-sulfated pentasaccharide Oligo-1 (B), or the 4-O-sulfated pentasaccharide Oligo-5 (C). ¹⁴C-labelled polymerization reaction products were isolated by gel filtration on a Superdex™ 75 column with 0.25 M NH₄HCO₃/0.7% propan-1-ol as the eluent. Numbered arrowheads 20K, 10K, 5K and 14 indicate the eluted position of 20, 10 and 5 kDa saccharides and tetradecasaccharides derived from chondroitin respectively. The total volume was at fraction ~60 (not shown).

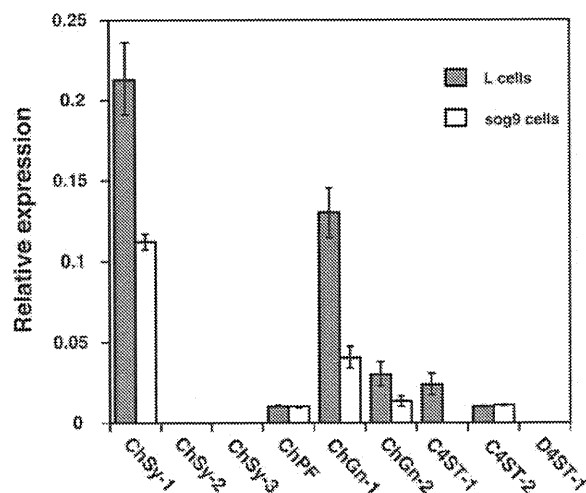


Figure S2 Expression levels of chondroitin synthase and sulfotransferase gene family in L and sog9 cells

Expression levels of chondroitin synthase and sulfotransferase gene family were normalized to those of GAPDH. Results are means ± S.E.M. for three experiments.

SUPPLEMENTARY METHODS

Polymerization assay and identification of polymerization reaction products

Any two of ChSy-1, ChSy-2, ChSy-3 and ChPF expression plasmids (3.0 μg each) were co-transfected into COS-1 cells on 100-mm-diameter plates using FuGENE® 6 as described previously [1–3]. At 2 days after transfection, 1 ml of the culture medium was collected and incubated with 10 μl of IgG–Sepharose for 1 h at 4°C. The beads recovered by centrifugation were washed with, and resuspended in, the assay buffer, and then tested for GalNAc transferase activity, as described [4]. Polymerization reactions using Oligo-1, Oligo-5 and Oligo-2 as acceptors were co-incubated in reaction mixtures containing the following constituents in a total volume of 20 μl: 1 nmol of Oligo-1, Oligo-2 or Oligo-5, 0.25 mM UDP-GalNAc, 0.25 mM UDP-[¹⁴C]GlcA (3 × 10⁵ d.p.m.), 100 mM Mes (pH 6.5), 10 mM MnCl₂ and 10 μl of the resuspended beads. The mixtures were incubated at 37 °C overnight. Products of the polymerization reactions were isolated by gel filtration on a Superdex™ 75 column with 0.25 M NH₄HCO₃/0.7% propan-1-ol as the eluent.

¹ These authors contributed equally to this work.

² To whom correspondence should be addressed (email kitagawa@kobepharm-u.ac.jp).

Table S1 Primers used for quantitative real-time RT-PCR

Target	5'-primer (5'→3')	3'-primer (5'→3')	Product length (bp)
ChSy-1	ACCACACATTGGCAAGT	TGTACCCCTTCTGTCTGTCA	158
ChSy-2	GACGATGTCACATCAAAGGTGATAA	CTGAAGATCATGCCAGGTC	170
ChSy-3	GCTTTCCTGAGTGCCCTT	CCAACAGGCCAGCTTAG	159
ChPF	CACGTACCAGGAGATTCAAGA	GAAGTAGTCCCAGCGCA	152
ChGn-1	TAAACAGCCCTGTGGAGAG	GTCGAAATAGGACAAGTCGC	185
ChGn-2	TTAATATCATTGTGCCACTTGCG	TAGAATAGACTTGACTTTAGATAGTCCTT	152
C4ST-1	ACCTCGTGGGCAAGTATGAG	TCTGGAAGAACTCCGTGGTC	141
C4ST-2	ATCAGCATCACCAGCAACA	TGTGGCCTGGAGAGAGAC	138
D4ST-1	GCCTCCTGAACAACGTG	TCTCCAAACTTGTACGGTAAGC	175
GAPDH	CATCTGAGGGCCCACTG	GAGGCCATGTAGGCCATGA	205

Quantitative real-time RT-PCR

Total RNA was extracted from L and *sog9* cells using TRIzol® reagent. The cDNA was synthesized from ~1 µg of total RNA using Moloney murine leukemia virus reverse transcriptase and a random primer according to the manufacturer's instructions. Quantitative real-time RT-PCR was performed using a FastStart DNA Master plus SYBR Green I (Roche) in a LightCycler ST300 (Roche). Specific primers for mouse chondroitin glycosyltransferase and sulfotransferase genes were designed using the LightCycler Probe Design Software version 3.3 (Roche). The expression level of the chondroitin glycosyltransferase or sulfotransferase mRNAs was normalized to that of the GAPDH transcripts. The primers used for quantitative real-time RT-PCR are shown in Supplementary Table S1.

REFERENCES

- 1 Kitagawa, H., Izumikawa, T., Uyama, T. and Sugahara, K. (2003) Molecular cloning of a chondroitin polymerizing factor that cooperates with chondroitin synthase for chondroitin polymerization. *J. Biol. Chem.* **278**, 23666–23671
- 2 Izumikawa, T., Uyama, T., Okuura, Y., Sugahara, K. and Kitagawa, H. (2007) Involvement of chondroitin sulfate synthase-3 (chondroitin synthase-2) in chondroitin polymerization through its interaction with chondroitin synthase-1 or chondroitin polymerizing factor. *Biochem. J.* **403**, 545–552
- 3 Izumikawa, T., Koike, T., Shiozawa, S., Sugahara, K., Tamura, J. and Kitagawa, H. (2008) Identification of chondroitin sulfate glucuronyltransferase as chondroitin synthase-3 involved in chondroitin polymerization: chondroitin polymerization is achieved by multiple enzyme complexes consisting of chondroitin synthase family members. *J. Biol. Chem.* **283**, 11396–11406
- 4 Kitagawa, H., Tsutsumi, K., Ujikawa, M., Goto, F., Tamura, J., Neumann, K. W., Ogawa, T. and Sugahara, K. (1997) Regulation of chondroitin sulfate biosynthesis by specific sulfation: acceptor specificity of serum β-GalNAc transferase revealed by structurally defined oligosaccharides. *Glycobiology* **7**, 531–537

Received 10 September 2010/29 November 2010; accepted 8 December 2010
Published as BJ Immediate Publication 8 December 2010, doi:10.1042/BJ20101456